iScience

CellPress
OPEN ACCESS

Article

Cocaine and habit training cause dendritic spine rearrangement in the prelimbic cortex

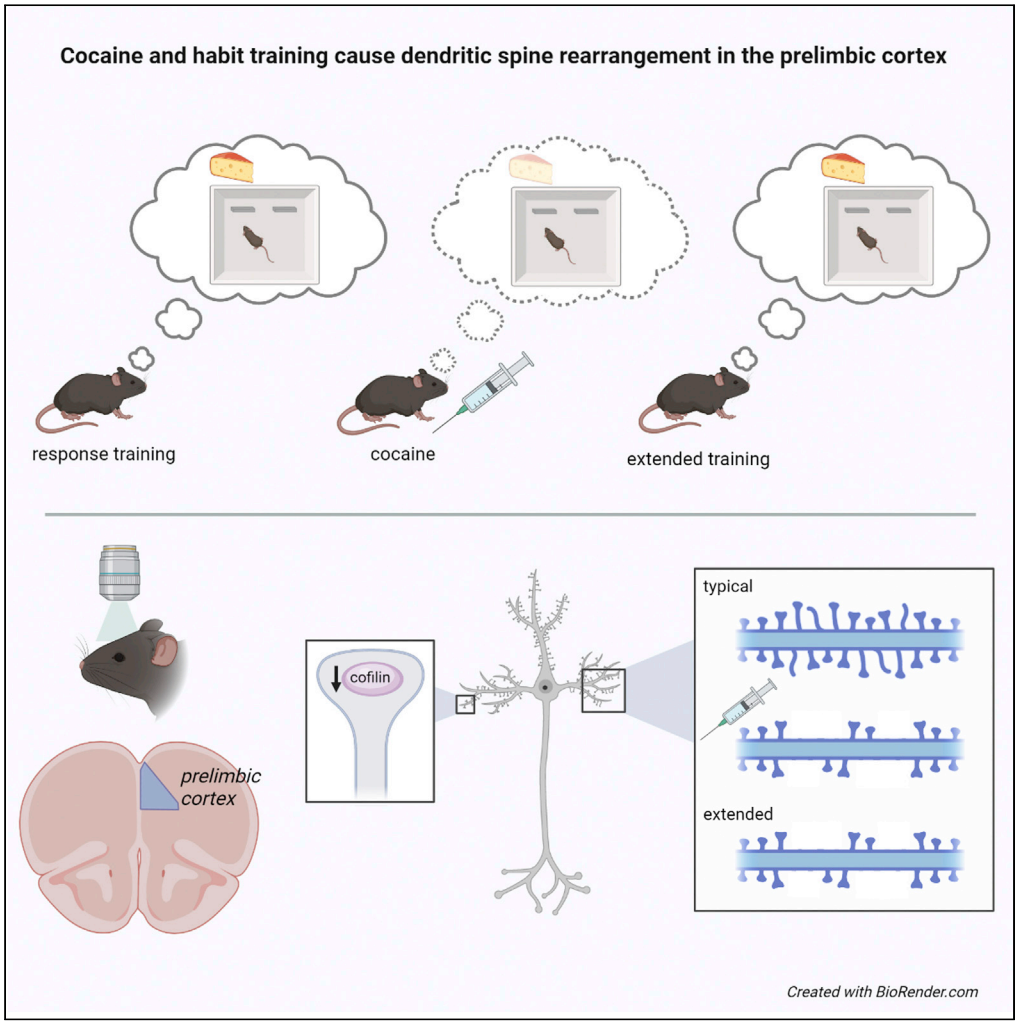

Michelle K. Sequeira, Andrew M. Swanson, Henry W. Kietzman, Shannon L. Gourley

shannon.l.gourley@emory.edu

Highlights

Acute cocaine obstructs flexible reward seeking by disrupting new memory formation

It also induces dendritic spine rearrangement on excitatory prelimbic cortex neurons

Extended habit training of drug-naive mice does the same

Thus, cocaine recapitulates neurobiological sequalae occurring in forming habits

Sequeira et al., iScience 26, 106240
April 21, 2023
https://doi.org/10.1016/j.isci.2023.106240

iScience

CellPress
OPEN ACCESS

Article

Cocaine and habit training cause dendritic spine rearrangement in the prelimbic cortex

Michelle K. Sequeira,[1,2] Andrew M. Swanson,[1,2] Henry W. Kietzman,[1,2] and Shannon L. Gourley[1,2,3,*]

SUMMARY

Successfully navigating dynamic environments requires organisms to learn the consequences of their actions. The prelimbic prefrontal cortex (PL) formulates action-consequence memories and is modulated by addictive drugs like cocaine. We trained mice to obtain food rewards and then unexpectedly withheld reinforcement, triggering new action-consequence memory. New memory was disrupted by cocaine when delivered immediately following non-reinforcement, but not when delayed, suggesting that cocaine disrupted memory consolidation. Cocaine also rapidly inactivated cofilin, a primary regulator of the neuronal actin cytoskeleton. This observation led to the discovery that cocaine also within the time of memory consolidation elevated dendritic spine elimination and blunted spine formation rates on excitatory PL neurons, culminating in thin-type spine attrition. Training drug-naive mice to utilize inflexible response strategies also eliminated thin-type dendritic spines. Thus, cocaine may disrupt action-consequence memory, at least in part, by recapitulating neurobiological sequalae occurring in the formation of inflexible habits.

INTRODUCTION

Navigating a changing environment requires one to extrapolate whether their behavior has consequences—a process often requiring the consolidation, retention, and later retrieval of new memories for sustained flexibility. A key brain region in this first step, consolidating expectations, is the prelimbic prefrontal cortex (PL) in rodents, which is functionally similar to aspects of the dorsal prefrontal cortex in humans.[1,2] In rodents, inactivation of the PL causes failures in selecting actions based on their consequences.[3–7] These deficiencies are attributable to disruption of memory consolidation—occurring in the minutes following new learning— as opposed to subsequent retrieval of that memory.[8–11]

Like PL inactivation, cocaine can cause failures in decision making requiring the assessment of goals and the likely outcomes of one's behavior.[12–14] While the majority of experiments concerning this phenomenon utilized chronic cocaine, some investigations reveal that pairing cocaine, as well as methamphetamine, with reward-seeking behaviors causes those behaviors to become habits, which are by definition insensitive to consequences.[15–17]

Here, we test the hypothesis that cocaine disrupts response flexibility by interrupting new memory consolidation, thus causing organisms to defer to familiar routines. We used a task in which mice first generate two food-reinforced nose poke behaviors equivalently, and then food associated with one response is no longer provided contingently. Optimally, mice update expectations and use this information to guide later choice—favoring the behavior that remained reinforced. As expected, cocaine disrupted new memory consolidation, occurring in the minutes following unexpected non-reinforcement, causing mice to maintain previously learned response strategies when tested later, drug free. Proteins that control the dendritic spine actin cytoskeleton—the structural lattice that controls the shape and stability of dendritic spines—were modified along the same timeline. Action-outcome learning, as assessed using both devaluation and contingency-based approaches, can be improved or impaired by manipulating spine dynamics in the PL during memory consolidation, strongly suggesting that dendritic spine plasticity optimizes new learning.[11] These insights together led us to next investigate cocaine-induced alterations in dendritic spine formation and elimination in the PL, again during the memory consolidation window. Cocaine caused spine attrition, preferentially affecting thin-type spines, transient extensions with the potential for synapse formation.[18,19]

[1]Graduate Program in Neuroscience, Emory National Primate Research Center, Departments of Pediatrics and Psychiatry and Behavioral Sciences, Emory University School of Medicine, Emory University, Atlanta, GA 30329, USA

[2]Children's Healthcare of Atlanta, Atlanta, GA 30329, USA

[3]Lead contact

*Correspondence: shannon.l.gourley@emory.edu

https://doi.org/10.1016/j.isci.2023.106240

A common notion is that addictive drugs hijack innate learning and memory processes. Following this logic, if cocaine-induced dendritic spine modifications are associated with disruptions in learning and memory, then schedules of reinforcement that cause drug-naive mice to be less flexible (*i.e.*, to use habitual response strategies) might modify dendritic spines in the PL in a similar fashion. Indeed, schedules of reinforcement that confer response inflexibility in drug-naive mice caused a loss of thin-type dendritic spines in the PL. Dendritic spine modifications were region specific and persistent and thus may be a mechanism by which the PL relinquishes control over reward-related behavior—due to training conditions or cocaine alike.

RESULTS

Cocaine disrupts memory consolidation

We hypothesized that cocaine disrupts memory consolidation, which would be expected to occur in the minutes following an opportunity to form new memories.[20] We trained mice to generate two instrumental responses for equally preferred foods (*e.g.*, left nose poke- > sweet grain pellet and right nose poke- > chocolate pellet) and then obstructed one response port and reduced the likelihood that responding on the other would be reinforced (Figure 1A). Successful memory consolidation is inferred when mice subsequently inhibit that response in a later choice test. By contrast, equivalent engagement of both behaviors reflects no new memory.

Treatment groups (vehicle or cocaine) were assigned by matching response rates during training, when mice were still drug naive (no main effect of group $F < 1$, no interactions $p > 0.26$) (Figure 1B). When one response was next no longer reinforced, response rates decreased as expected, again without group differences (main effect of time $F_{(4,88)} = 22.20$, $p < 0.001$, other $F < 1$) (Figure 1C). Indeed, group differences were never identified during this session; thus, these data will not be shown in subsequent figures. Vehicle or cocaine was delivered immediately after this session. During a probe test conducted the following day and repeated the day after that to determine the stability of response patterns, mice that had received vehicle preferentially responded on the aperture most likely to be reinforced, reflecting new memory. Meanwhile, mice exposed to cocaine exhibited non-preferential responding (drug × aperture interaction $F_{(1,22)} = 7.58$, $p = 0.01$) (Figure 1D). Thus, cocaine obstructed new action-consequence memory.

New learning involves the consolidation and retrieval of memory. To test the hypothesis that cocaine disrupted memory consolidation, in particular, we compared the impact of immediate post-training vs. delayed cocaine injections. If cocaine disrupts *consolidation*, then delayed injections will have no effects. We first replicated our experiment above and added a group in which injection was delayed by 30 min. The two vehicle control groups did not differ and were combined. Groups did not differ during training (no main effect of group $F < 1$, no interactions $F < 1$) (Figures 2A and 2B). Then, one response ceased to be reinforced, and vehicle or cocaine was delivered. During a probe test the next day, vehicle control mice and mice given a delayed cocaine injection preferentially engaged the response most likely to be reinforced, evidence of successful memory consolidation (Figure 2C). When cocaine was paired with the non-reinforced condition, however, mice failed to modify behavior, evidence of no new memory (drug condition × aperture interaction $F_{(2,23)} = 3.46$, $p = 0.049$) (Figure 2C).

Thus, cocaine appears to disrupt instrumental memory consolidation. To further substantiate this perspective, we gave another group of mice injections that were delayed by 4 or 19 h following the non-reinforced session (timeline in Figure 2A). These delayed injections again had no effects (no effect of delayed drug group during response acquisition $F < 1$, no interactions $p > 0.2$; probe test main effect of aperture $F_{(1,21)} = 18.14$, $p < 0.001$, no interactions or effect of delayed drug group $F < 1$) (Figures 2D and 2E). Thus, cocaine blocks instrumental memory consolidation, occurring within 30 min following an opportunity to form new associations.

Given that excitatory plasticity in the PL is necessary for action-outcome memory (see introduction), we next reasoned that decreasing neuronal activity in the PL should recapitulate the effects of acute cocaine. To test this prediction, we infused mice with either control viral vectors or viral vectors expressing CaMKII-driven Gi-coupled designer receptor exclusively activated by designer drugs (DREADDs) bilaterally into the PL. Histological analysis revealed that all mice had transduced cells in the PL across the rostral-caudal axis, with some spread into the medial orbitofrontal cortex in some mice (Figures 3A and 3B). We did not detect obvious differences between mice with small or larger infusion sites, consistent with evidence that

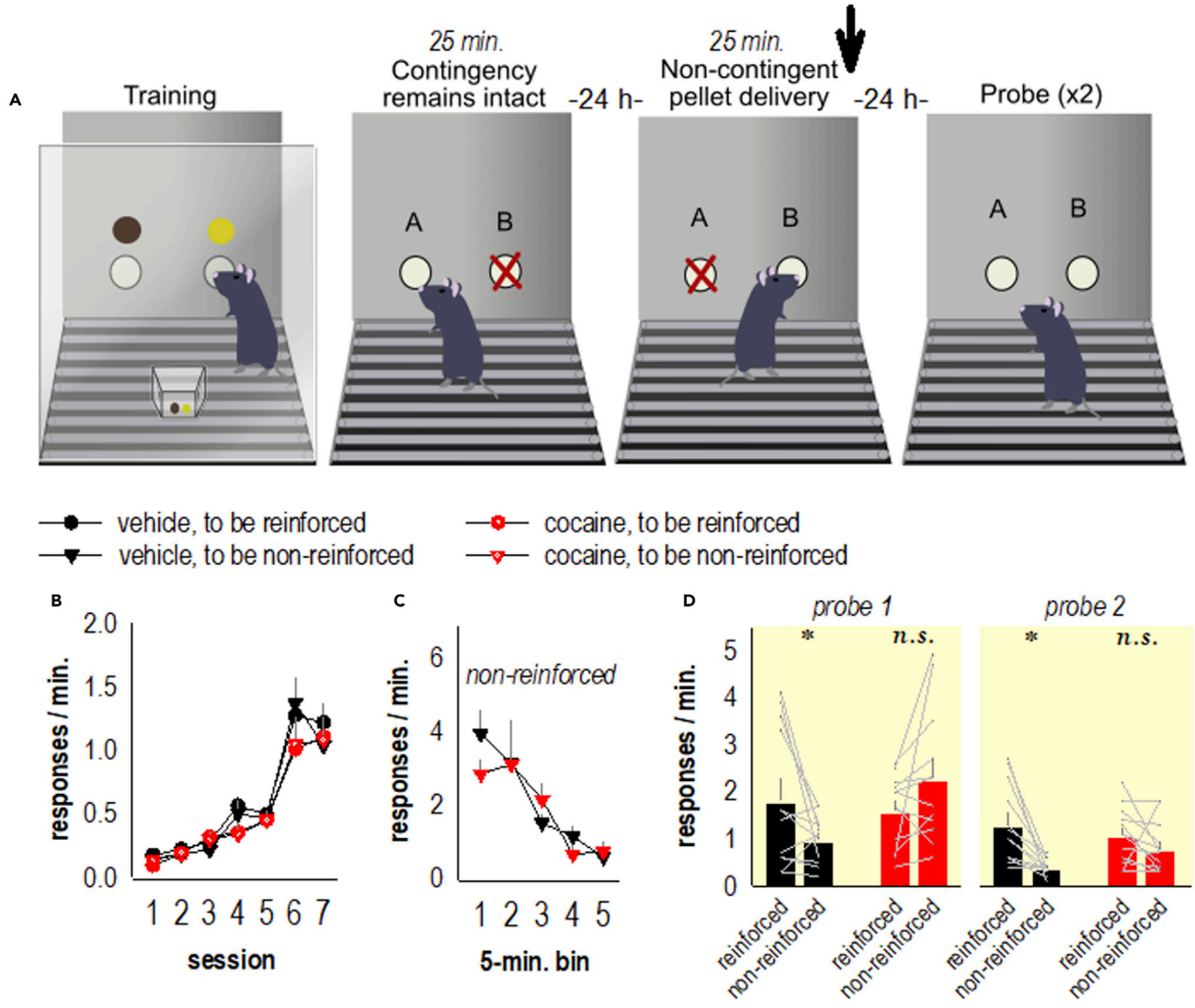

Figure 1. Cocaine disrupts memory for action outcomes

(A) Schematic and timing of task: mice were trained to respond at two nose poke ports for food—sweetened grain or chocolate pellets. Then, one port was occluded, and responding on the other remained reinforced. Next, the contingency between the other response and the outcome was violated by providing the associated pellet non-contingently, and responding was not reinforced. Immediately following this session, mice received an injection of cocaine. The next day, a brief probe test was conducted when mice were drug free, and response preference was measured. The probe test was repeated the next day.

(B) Response acquisition curve, with no differences between groups that would later receive vehicle vs. cocaine. There were also no differences between the response that would remain reinforced and the response that would later be non-reinforced.

(C) Response rates declined when responses were not reinforced and pellet delivery was non-contingent. An injection of vehicle or cocaine immediately followed.

(D) The following day, vehicle-treated mice preferred the reinforced response, while cocaine blocked new learning, causing mice to respond equally on both ports, as during training. This pattern persisted in a second probe test (n = 12/group). Bars and symbols: Mean + SEMs. Gray lines represent individual mice, *p < 0.05. "n.s." refers to non-significant.

medial orbitofrontal cortex does not obviously control responding in a very similar task.[21] We also found no effects of viral vectors in response acquisition (no main effect of group or interactions $F < 1$) (Figure 3C). We then administered the DREADD ligand clozapine N-oxide (CNO) prior to the 25-min "non-reinforced" session, given that CNO appears to require roughly 30 min to cross the blood-brain barrier.[22] Mice also received an injection immediately following the procedure: either vehicle or cocaine, in order to compare the degree to which Gi-DREADDs activation recapitulated the effects of cocaine (timeline in Figure 3B). In a probe test the following day, control mice preferentially engaged the response most likely to be

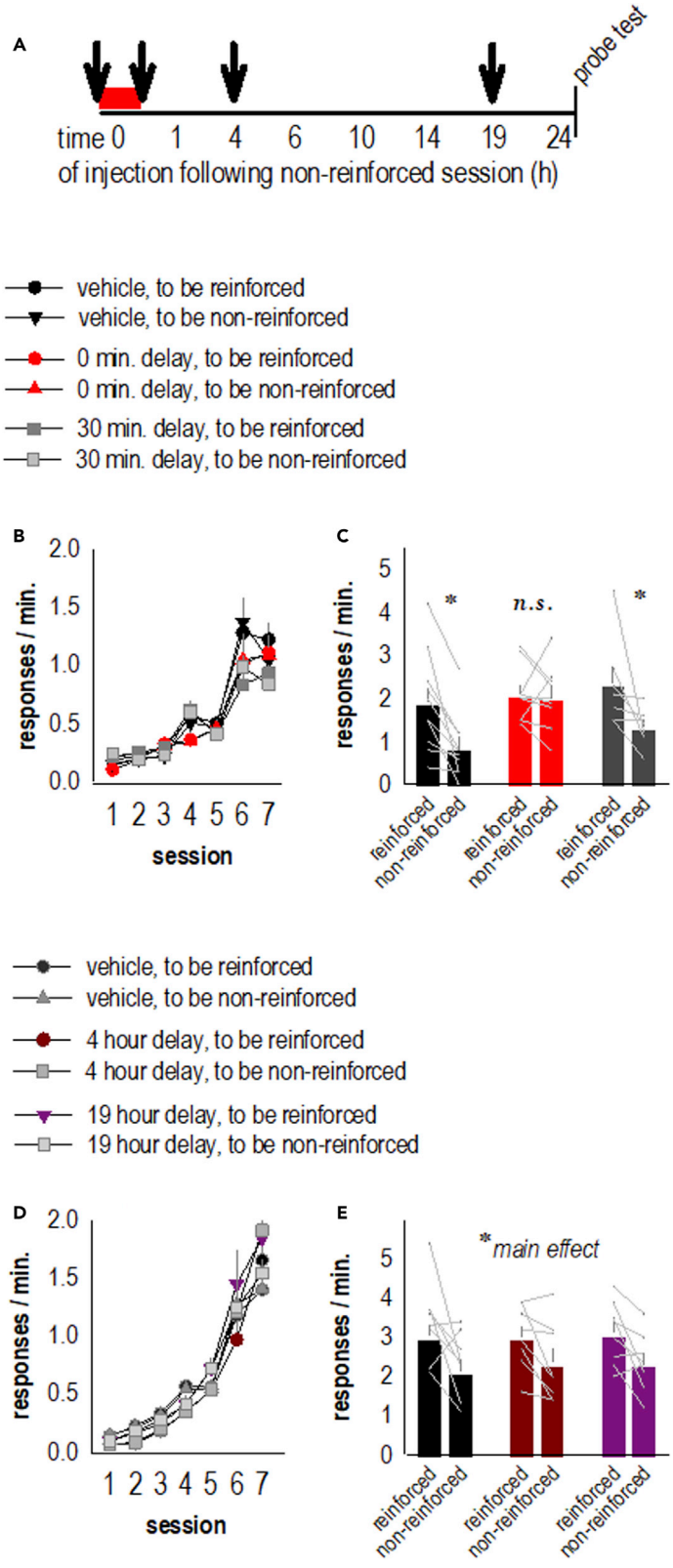
A
probe test
time 0 1 4 6 10 14 19 24
of injection following non-reinforced session (h)
vehicle, to be reinforced
vehicle, to be non-reinforced
0 min. delay, to be reinforced
0 min. delay, to be non-reinforced
30 min. delay, to be reinforced
30 min. delay, to be non-reinforced
B
responses / min.
2.0
1.5
1.0
0.5
0.0
1 2 3 4 5 6 7
session
C
responses / min.
5
4
3
2
1
0
*
n.s.
*
reinforced
non-reinforced
reinforced
non-reinforced
reinforced
non-reinforced
vehicle, to be reinforced
vehicle, to be non-reinforced
4 hour delay, to be reinforced
4 hour delay, to be non-reinforced
19 hour delay, to be reinforced
19 hour delay, to be non-reinforced
D
responses / min.
2.0
1.5
1.0
0.5
0.0
1 2 3 4 5 6 7
session
E
responses / min.
5
4
3
2
1
0
*main effect
reinforced
non-reinforced
reinforced
non-reinforced
reinforced
non-reinforced

Figure 2. Cocaine disrupts memory consolidation

(A) Timing of cocaine injection relative to the end of a test session when a familiar action was not reinforced (arrows). Zero refers to immediately following that session; other injections were at 30 min (end of red bar), 4 h, or 19 h following the non-reinforced session. Response preference was tested the next day in a probe test.

(B) Response acquisition curves, with no differences between groups that would later receive vehicle or cocaine.

(C) Acute cocaine blocked new learning, as indicated by a failure to prefer the reinforced behavior during the probe test, but injection delayed by 30 min had no effect (n = 10 control, 9 cocaine, 7 delayed cocaine).

(D) We next tested response strategies after longer delays. Response acquisition curves.

(E) Injections delayed by 4 and 19 h again had no effects, given that all groups preferred the behavior that was reinforced (n = 8/group). Thus, cocaine disrupts new memory consolidation, occurring within 30 min following new learning. Bars and symbols: mean + SEMs. Gray lines represent individual mice, *p < 0.05. "n.s." refers to non-significant.

reinforced—evidence of new learning (Figure 3D; control groups are collapsed for simplicity). Meanwhile, both cocaine and Gi-DREADDs interfered with new memory [drug condition × aperture interaction $F_{(2,23)}$ = 4.12, p = 0.03] (Figure 3D), replicating the effects of cocaine described in Figures 1 and 2 and the effects of chemogenetically silencing excitatory PL neurons described previously.[11] This conclusion can be further appreciated by comparing the ratio of reinforced/non-reinforced responses (Figure 3E). In this case, 1 reflects no response preference, and scores >1 would be interpreted as successful memory consolidation. Both cocaine and Gi-DREADDs mice generated preference ratios of ∼1, evidence of no new learning (H_2 = 6.32, p = 0.04) (Figure 3E).

Discerning rapid actions of cocaine

To summarize thus far, cocaine disrupts action-consequence memory consolidation occurring within 30 min following new learning. This led to the following question: what are the rapid impacts of cocaine, specifically, those occurring within 30 min of administration? We began by quantifying several proteins in the PL 30 min following an acute cocaine injection, starting with the immediate-early gene, c-fos. C-fos levels were lower in the cocaine group (Figure 4A; see Table 1 for means, SEMs, and statistics for all western blotting experiments; see Table 2 for antibody information). Of the several other targets investigated, only one more was altered: Cocaine also elevated phosphorylation of a master cytoskeletal regulatory protein cofilin (Figure 4A), which inactivates the protein.

To determine the degree to which these effects were associated with rapidly acting acute cocaine, we next measured cofilin phosphorylation in mice exposed to 2 weeks of cocaine or ketamine as a positive control[23] (Figure 4B). Only ketamine elevated phosphorylation (drug × time interaction $F_{(2,33)}$ = 3.47, p = 0.04, no main effect of time $F_{(1,33)}$ = 2.08, p = 0.16, main effect of drug $F_{(2,33)}$ = 3.51, p = 0.04) (Figure 4B). To confirm that we could detect *some* effect of repeated cocaine, we also measured cortactin, another cytoskeletal regulatory protein thought to be involved in cocaine-induced neuronal remodeling.[15,24] In this case, both cocaine and ketamine increased phospho-cortactin (drug × time interaction $F_{(2,34)}$ = 3.47, p = 0.04, main effect of time $F_{(1,34)}$ = 12.58, p = 0.001, no main effect of drug $F_{(2,34)}$ = 1.26, p = 0.30) (Figure 4B).

Cocaine induces rapid dendritic spine rearrangement in the PL

Thus far, we report that acute cocaine can disrupt instrumental memory consolidation, a process that requires the PL, simultaneously modifying the cytoskeletal regulatory element cofilin. We hypothesized that acute cocaine would affect dendritic spine plasticity in the PL, and importantly, within 30 min of injection, consistent with the timing in which it disrupts PL-dependent memory. We first deployed *in vivo* imaging to visualize rapid changes in dendritic spine turnover, if any.

The skull was thinned in anesthetized mice expressing Yellow Fluorescent Protein in layer V neurons. Mice were then placed on a microscope stage to obtain a field of view that contained distinct, resolvable dendritic segments, specifically within the rostral PL, where dendrites extend to the surface (see for reference the rostral-most section in Figure 3A). Immediately prior to the first imaging time point, an intraperitoneal (*i.p.*) injection of vehicle was administered. Images were collected 0, 15, and 30 min afterward. Next, cocaine was administered *i.p.*, again with images collected 0, 15, and 30 min afterward. Gross dendritic spine densities did not differ between drug conditions (no drug × time interaction $F_{(2,16)}$ = 2.10, p = 0.15, no main effect of time or drug F < 1) (Figures 5A and 5B). To evaluate dendritic spine turnover rates, we calculated the number of spines gained or lost relative to the total number of spines present at the previous time point in the imaging session.[25] Cocaine blunted the rate at which new spines appeared (main effect of drug $F_{(1,8)}$ = 12.40, p = 0.03, no main effect of time or interaction p > 0.05) (Figure 5C). When we analyzed dendritic spines

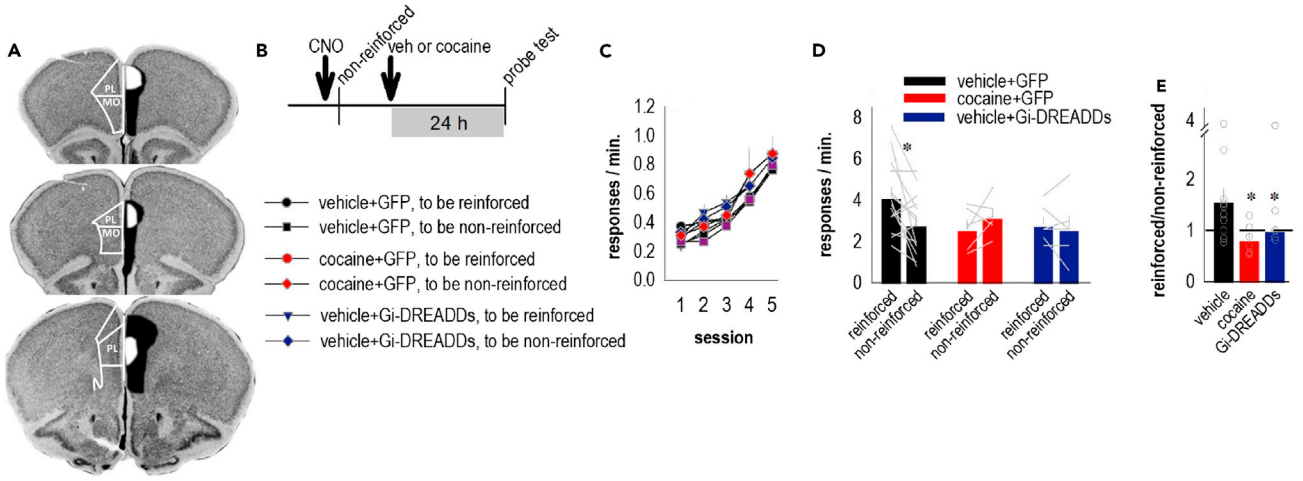

Figure 3. Memory for action outcomes requires the PL

(A) Viral-driven Gi-DREADDs or a control viral vector expressing GFP was placed bilaterally in the PL. Viral vector spread is depicted in one hemisphere from the *Mouse Brain Atlas*, with black representing the largest spread and white, the smallest, and anatomical boundaries indicated in the contralateral hemisphere.

(B) Timeline. The DREADD ligand CNO was delivered immediately before the non-reinforced session, allowing time for the CNO to cross the blood-brain barrier and bind to DREADDs following the session. Vehicle or cocaine was also delivered immediately following the non-reinforced session, as in prior figures. Choice was assessed in a probe test 24 h later.

(C) Response acquisition curves, with no differences between groups.

(D) Silencing excitatory neurons in the PL via Gi-DREADDs blocked new learning about action outcomes, phenocopying the effects of acute cocaine exposure.

(E) The same data can be converted to preference scores (responses on the ports associated with the reinforced/non-reinforced conditions), such that scores >1 reflect new learning, while scores of ~1 reflect no learning. Again, Gi-DREADDs in the PL and acute cocaine blocked new learning (n = 14 control, 6 cocaine, 6 Gi-DREADDs). Bars and closed symbols: mean + SEMs. Open symbols and gray lines represent individual mice, *p < 0.05.

that disappeared, cocaine caused significantly more spines to disappear by 30 min (drug × time interaction $F_{(1,8)} = 34.60$, $p < 0.01$, no main effect of time or drug $p > 0.05$) (Figure 5D). Thus, cocaine rapidly—within 30 min—slowed the rate of new spine formation and elevated the rate of spine loss.

Dendritic spines can be classified based on their shape—stubby, thin, and mushroom—with thin-type spines being the most dynamic and labile. This pattern of slowed spine formation and elevated spine loss following cocaine led to the hypothesis that labile, thin-type spines would differ between vehicle vs. cocaine-treated mice, a pattern that could be masked in measures of gross spine densities. Thus, we next turned to dendritic spine classification to quantify the densities of different spine subtypes. Spine classification is generally not applied to *in vivo* imaging experiments because of modest image artifacts due to respiration. Thus, we turned to *ex vivo* imaging and imaged PL neurons 30 min after cocaine to mirror the *in vivo* investigation above. We additionally imaged neurons from brains collected 24 h after vehicle or cocaine to determine whether any morphological changes were persistent (Figure 6A). There was no effect of cocaine on stubby spines at any time (no main effect $F_{(1,19)} = 0.31$, $p = 0.58$, no interaction $F < 1$), mushroom spines (no main effect $F_{(1,19)} = 3.42$, $p = 0.08$, no interaction $F < 1$), or thin-type spines (main effect $F_{(1,19)} = 1.11$, $p = 0.31$, no interaction $F_{(1,19)} = 2.24$, $p = 0.15$) (Figure 6B). Stubby spine densities were lower at the 24 h time point (main effect of time $F_{(1,19)} = 9.82$, $p = 0.01$), but timing had no impact on mushroom ($F_{(1,19)} = 1.09$, $p = 0.31$) or thin-type spines ($F_{(1,19)} = 0.44$, $p = 0.52$) (Figure 6B). Interestingly, though, despite no gross changes in individual spine densities, cocaine decreased the thin:non-thin spine ratio, indicating that cocaine causes rapid changes in spine compositions that bias spine types away from labile thin-type spines, characterized by their capacity for synapse formation (main effect of drug $F_{(1,19)} = 9.40$, $p = 0.006$, all other Fs<1) (Figure 6C).

Schedules of reinforcement that confer response inflexibility modify dendritic spine compositions on excitatory neurons in the PL

It is commonly postulated that addictive drugs hijack innate learning and memory systems. Following this logic, we hypothesized that training conditions that promote response inflexibility might modify dendritic

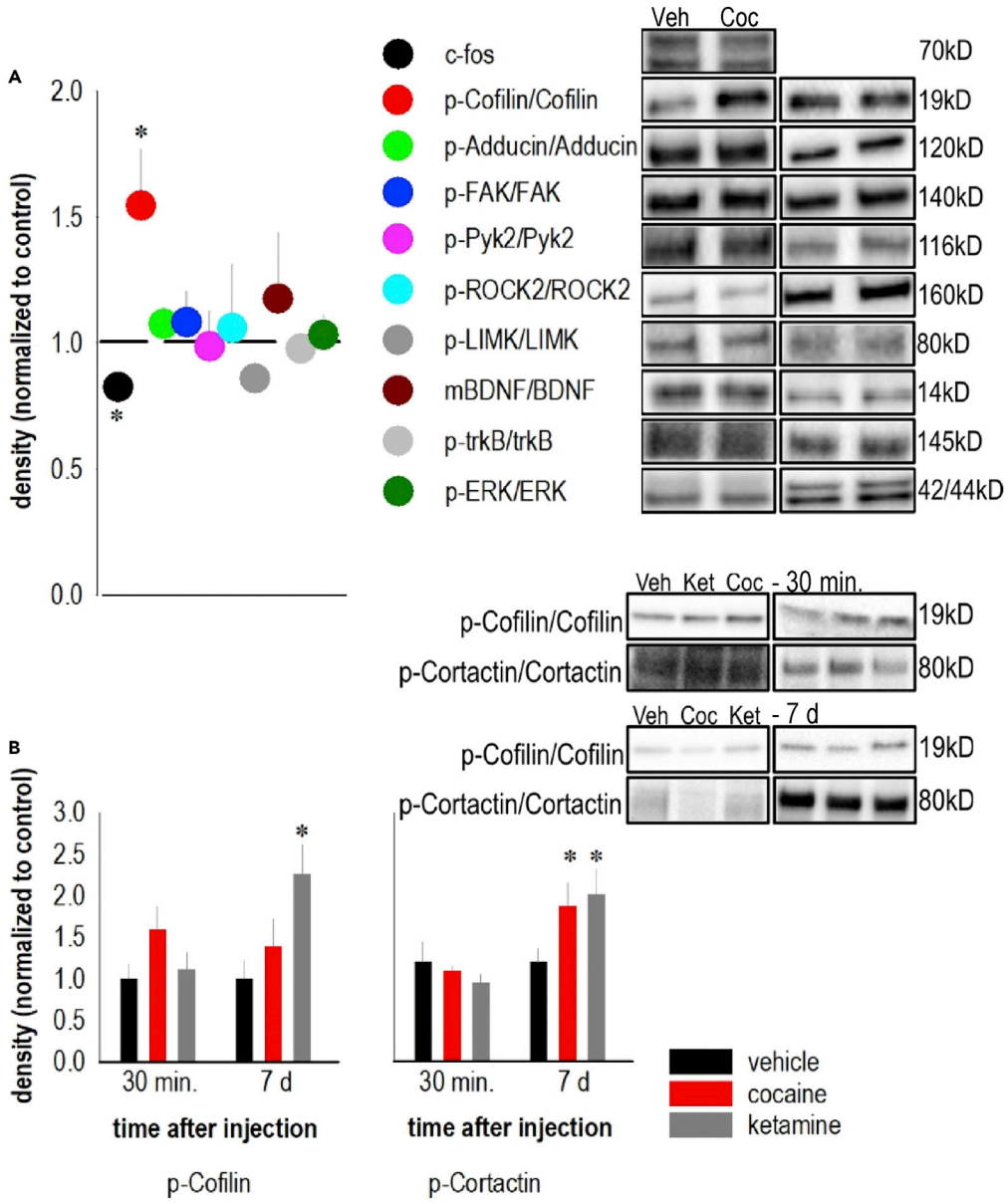

Figure 4. Cocaine rapidly alters immediate-early gene levels and cofilin activity in the PL

(A) A single injection of cocaine was delivered, and brains were collected 30 min later to ascertain the rapid actions. Cocaine decreased c-fos protein and increased cofilin phosphorylation at ser3 in the PL. Several other proteins were unaffected (n = 9–12/group; normalized to mean of control mice at dashed line). Proteins are color coded, and they are presented in the same order as listed in the legend. Representative blots are adjacent to the corresponding protein in the legend, with molecular weights indicated, vehicle lane first. The phosphorylated protein signal, when relevant, is represented first.

(B) Separate mice were treated with cocaine daily for 2 weeks and euthanized 30 min or 7 days later. p-cofilin trended higher. As a positive control, other mice were given repeated ketamine, which increased p-cofilin with time. Another protein, p-cortactin, increased with both repeated cocaine and ketamine (n = 6–8/group). Representative blots are adjacent. Bars and symbols: mean + SEMs, *p $\leq$ 0.05. Gel images were cropped to highlight the labeled proteins. Proteins were detected at expected molecular weights indicated.

spines in the PL in a fashion similar to cocaine. To investigate this possibility, we trained drug-naive mice to nose poke using either random ratio (RR) or random interval (RI) schedules of reinforcement because RR training promotes flexible responding, while RI training facilitates the development of habitual, inflexible

Table 1. Effects of acute cocaine on protein content in the mouse PL

Protein	Group	Mean	SEM	*t*	*p*
C-fos	Vehicle	1.00	0.06	2.51	0.02
	Cocaine	0.83	0.03		
p-Cofilin/Cofilin	Vehicle	1.00	0.12	−2.08	0.05
	Cocaine	1.55	0.22		
p-Adducin/Adducin	Vehicle	1.00	0.04	−0.91	0.37
	Cocaine	1.08	0.06		
p-FAK/FAK	Vehicle	1.00	0.08	−0.53	0.60
	Cocaine	1.08	0.13		
p-Pyk2/Pyk2	Vehicle	1.00	0.25	0.05	0.96
	Cocaine	0.99	0.14		
p-ROCK2/ROCK2	Vehicle	1.00	0.14	−0.19	0.86
	Cocaine	1.06	0.28		
p-LIMK/LIMK	Vehicle	1.00	0.08	1.29	0.23
	Cocaine	0.86	0.07		
mBDNF/BDNF	Vehicle	1.00	0.24	−0.48	0.64
	Cocaine	1.18	0.29		
p-TrkB/TrkB	Vehicle	1.00	0.06	0.30	0.77
	Cocaine	0.98	0.05		
p-ERK/ERK	Vehicle	1.00	0.06	−0.33	0.75
	Cocaine	1.03	0.08		

Means, SE, and statistical reporting are reported for the proteins measured in Figure 4A.

responding.[26] Response rates did not differ between groups during response acquisition (no main effect of group or interactions $F < 1$) (Figure 7A), but as expected, the RR group reduced responding following a "non-reinforced" test session, while the RI group was insensitive to contingency changes (schedule × aperture interaction $F_{(1,16)} = 4.45$, p = 0.05) (Figure 7B).

Mice were euthanized either within 30 min following the non-reinforced session (during the consolidation of new instrumental memory) or 3 days following the probe test. Regardless of timing, thin-type spine densities in the PL were lower in the RI group (main effect of schedule $F_{(1,31)} = 5.76$, p = 0.02, no main effect of time or interaction $F < 1$) (Figure 7C). By contrast, mushroom-shaped spines did not differ (all $F < 1$), and stubby-type spines were modestly impacted by the timing of euthanasia, slightly elevated in the group euthanized days after conditioning (main effect of time $F_{(1,31)} = 6.77$, p = 0.01, no main effect of schedule or interaction $F < 1$) (Figure 7C). Thus, RI training induced behavioral and dendritic spine modifications reminiscent of cocaine exposure. Further solidifying this point, RI training also reduced the thin:non-thin spine ratios, as with cocaine exposure (main effect of schedule $F_{(1,28)} = 6.23$, p = 0.019; no main effect of time $F_{(1,28)} = 3.723$, p = 0.064, no interaction $F < 1$) (Figure 7D).

In contrast to the PL, dendritic spine densities on hippocampal CA1 neurons in the RR- and RI-trained mice did not differ between groups (stubby: $t_{16} = -0.33$, p = 0.75; mushroom $t_{16} = 0.35$, p = 0.73; thin $t_{16} = 1.58$, p = 0.13) (Figure 7E), nor did the thin:non-thin spine ratios [$t_{16} = 1.226$, p = 0.238] (Figure 7F). This pattern suggests that training-induced anatomical modifications are at least somewhat region specific.

To summarize, the formation of inflexible responding via RI training appears to be associated with selective reduction of thin-type spines in the PL, consistent with the effects of acute cocaine exposure. An alternative perspective is that RR training *elevated* spine densities. To test this possibility, we next trained mice to acquire food reinforcers. A separate group of mice was similarly food-restricted and placed daily in the operant conditioning chambers, but food pellets were delivered non-contingently at a rate yoked to a mouse responding for food reinforcers. These mice were thus exposed to food restriction, handling, the testing chambers, and food pellets but did not learn that nose poking was reinforced. While all mice

Table 2. Antibodies used in this report

Antibody	Immunogen	Host	Manufacturer	Product #	Concentration
anti-*c*-fos	N-terminus domain	Rabbit	Santa Cruz Biotechnology	sc-52	1:500
anti-*p*-Cofilin	Proprietary sequence	Rabbit	Cell Signaling Technology	3311S	1:250
anti-Cofilin	N-terminus domain	Rabbit	ECM Biosciences	CP1131	1:1000
anti-*p*-Adducin	aa 656-668	Rabbit	Millipore Sigma	06-820	1:5000
anti-Adducin	aa 13-51	Mouse	Santa Cruz Biotechnology	sc-376063	1:500
anti-*p*-FAK	Proprietary sequence	Rabbit	Abcam	ab81298	1:1000
anti-FAK	Proprietary sequence	Rabbit	Cell Signaling Technology	3285S	1:1000
anti-*p*-Pyk2	Proprietary sequence	Rabbit	Cell Signaling Technology	3291S	1:1000
anti-Pyk2	N-terminus domain	Rabbit	Cell Signaling Technology	3292S	1:1000
anti-p-ROCK2	Proprietary sequence	Rabbit	GeneTex	GTX122651	1:1000
anti-ROCK2	aa 1-100	Rabbit	Abcam	ab71598	1:500
anti-*p*-LIMK	Proprietary sequence	Rabbit	Cell Signaling Technology	3841S	1:500
anti-LIMK	aa 561-638	Rabbit	Santa Cruz Biotechnology	sc-5577	1:500
anti-BDNF	Proprietary sequence	Rabbit	Abcam	ab108319	1:500
anti-*p*-TrkB	Proprietary sequence	Rabbit	Cell Signaling Technology	4621S	1:100
anti-TrkB	Proprietary sequence	Rabbit	Cell Signaling Technology	4603S	1:500
anti-*p*-ERK	Proprietary sequence	Rabbit	Cell Signaling Technology	9101S	1:2000
anti-ERK	C-terminus domain	Rabbit	Cell Signaling Technology	9102S	1:2000
anti-*p*-Cortactin	Proprietary sequence	Rabbit	Cell Signaling Technology	4569S	1:100
anti-Cortactin	aa 309-499	Mouse	Santa Cruz Biotechnology	sc-55578	1:1000

Antibody information is reported.

investigated the nose poke apertures during the initial 2 training sessions regardless of group, nose poking in food-reinforced mice subsequently increased as expected, while exploration of the nose poke recesses in the non-reinforced mice dropped, also as expected (training condition × day interaction $F_{(4,44)} = 6.41$, $p < 0.001$) (Figure 7G).

When one response was no longer reinforced, trained mice then preferentially performed the other (reinforced) nose poke, evidence of successful memory consolidation. Again, the matched, "no training" group generated virtually no nose pokes at all, as expected (training condition × aperture interaction $F_{(1,11)} = 57.48$, $p < 0.001$) (Figure 7H). These behavioral data were first reported by us in a different report,[27] in which case, neurons in other brain regions were analyzed. Here, in the PL, dendritic spine densities did not differ between groups (thin-type $t_{11} = -1.26$, $p = 0.24$; mushroom $t_{11} = -0.16$, $p = 0.87$; stubby $t_{11} = -0.36$, $p = 0.72$) (Figure 7I), nor did the thin:non-thin spine ratios ($t_{11} = 0.434$, $p = 0.672$) (Figure 7J). Thus, instrumental conditioning did not obviously stimulate dendritic spinogenesis in the PL.

DISCUSSION

Here we investigated the ability of mice to select actions based on their consequences and how cocaine disrupts this process. Mice were trained to respond for food reinforcers, and then reinforcers were unexpectedly withheld. Typical mice subsequently modified responding, no longer engaging the non-rewarded response during later probe tests. This memory for action-consequence relationship was vulnerable to disruption by cocaine when it was delivered immediately following the non-reinforcement session but not when injection was delayed by as little as 30 min. This pattern indicates that cocaine disrupted new memory consolidation and led us to ask the following: what are the rapid consequences of cocaine in the brain, occurring within 30 min? Cocaine elevated dendritic spine elimination and blunted spine formation rates on excitatory layer V neurons in the PL along this time course, culminating in a reduction in the proportion of spines that were thin in shape. Similarly, drug-naive mice trained to utilize inflexible response strategies had fewer thin-type dendritic spines on excitatory neurons in the PL. Thin-type spines are labile

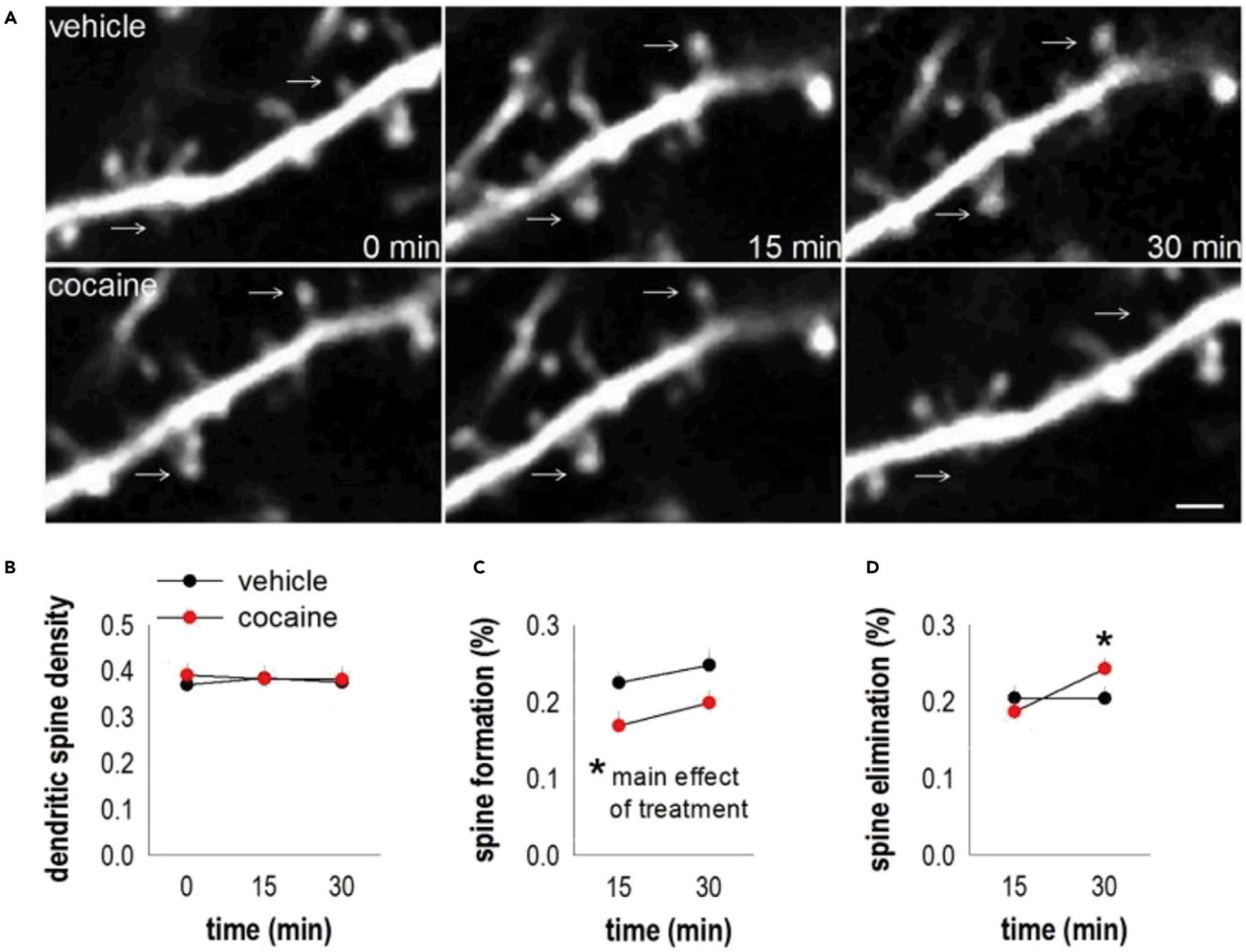

Figure 5. *In vivo* imaging reveals that cocaine rapidly suppresses dendritic spine formation and elevates elimination on excitatory PL neurons

(A) Representative images depicting dendrites in the PL. The same dendrites were imaged across time and anatomically corresponded with the rostral-most sections in Figure 3.

(B) Gross dendritic spine densities (spines/μm) did not differ 0, 15, and 30 min after vehicle vs. cocaine.

(C) However, cocaine blunted dendritic spine formation and (D) accelerated dendritic spine elimination. Here, the 15 and 30 min time points are normalized to the baseline, at 0 min (n = 9/condition). Symbols: mean + SEMs, *p < 0.05. Scale = 2 μm.

and have the potential to house stable synapses.[19,28] Thus, their constraint in the PL may be a mechanism by which cocaine or environmental circumstances limit action-outcome control over behavior.

Cocaine weakens memory consolidation and reorganizes dendritic spines

Cocaine disrupts learning regarding the predictive relationship between actions and their consequences in both rodents[12] and humans.[14] The majority of prior experiments exposed organisms to repeated cocaine and then assessed flexible behavior later, revealing long-term consequences of historical drug exposure, biasing reward-seeking behaviors toward inflexible habits. However, pairing cocaine with a given behavior also causes that behavior to become habitual, implying loss of action-outcome memory,[15–17] and our goal was to understand mechanistic factors. Mice were first trained to generate two reinforced behaviors. Then, the predictive relationship between one behavior and its outcome was violated by providing the associated food pellet non-contingently, and responding was not reinforced. Response preference was assessed the following day. Cocaine given immediately following the non-reinforced session occluded new memory, causing mice to defer to familiar response strategies. Injections delayed by 30 min, 4 h, or 19 h had no effects. This experimental design—drug treatment immediately following a learning event compared to delayed treatment—is a classical approach to investigating memory consolidation, which occurs in the

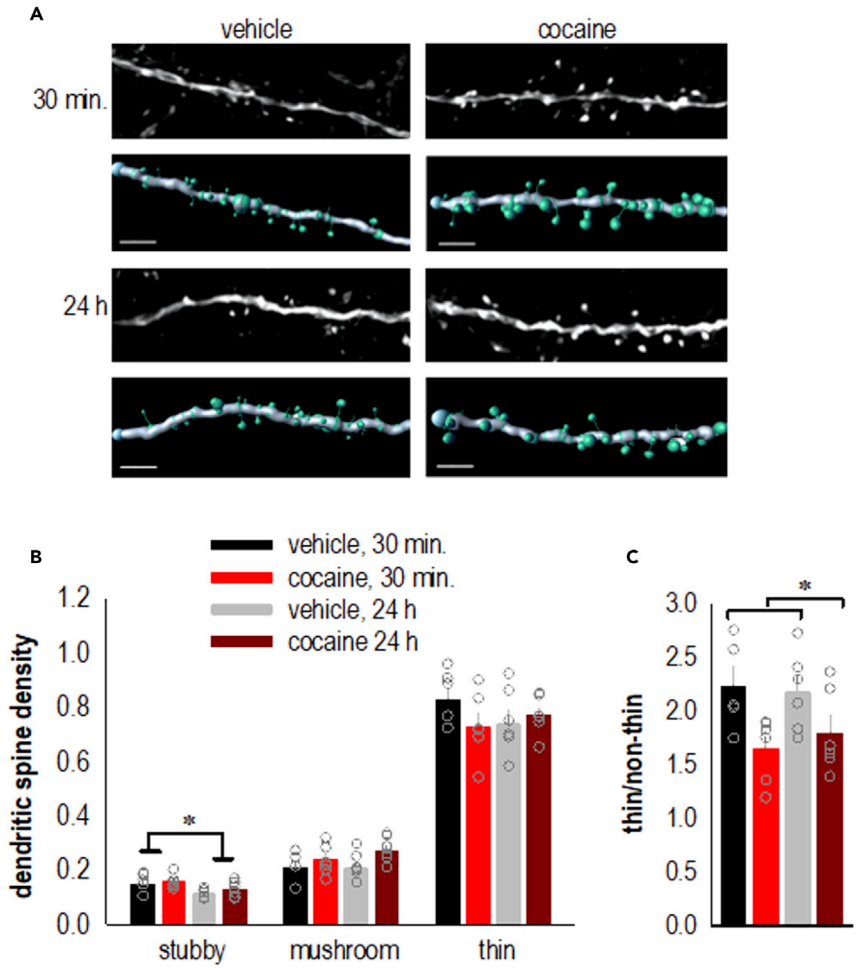

Figure 6. *Ex vivo* imaging reveals that cocaine modifies spine types on excitatory PL neurons

(A) *Ex vivo* imaging was used to visualize and reconstruct dendrites and classify dendritic spines types within the PL, anatomically defined as in Figure 3.

(B) Cocaine did not grossly change dendritic spine densities (spines/μm) on excitatory PL neurons, and there was a modest loss of stubby-time spines with time.

(C) Cocaine, however, decreased the thin:non-thin spine type ratio (n = 5,6/group). Bars: means + SEMs. Open symbols represent individual mice, *p < 0.05. Scale = 2 μm.

minutes following new learning. By avoiding treating mice *before* the non-reinforced session, we avoided impacting the *acquisition* of new associations, and by including *delayed* treatment, we can conclude that cocaine disrupts memory consolidation rather than non-specific retention processes.

We hypothesized that cocaine-induced behavioral patterns were associated with modifications to the PL, given that the PL is necessary for action-outcome memory[6] and is modulated by cocaine.[29] Given that memory was subjected to disruption within a 30-min period, we focused on this time window. Acute cocaine reduced immediate-early gene expression and the rate of dendritic spine proliferation in the PL, ultimately culminating in thin-type spine attrition. The pattern was notable because action-outcome memory requires projections from the mediodorsal thalamus to PL,[30] which would preferentially terminate on layer V neurons, imaged here.[31]

The effects of cocaine on dendritic spines might be surprising to some readers, given that cocaine is often thought to cause dendritic spine *proliferation* in the medial prefrontal cortex. For instance, Muñoz-Cuevas et al.[32] used *in vivo* fluorescence-based dendritic spine imaging and reported that acute cocaine *increases* prefrontal cortical dendritic spine density and the rate of new spine formation within 2 h after injection.

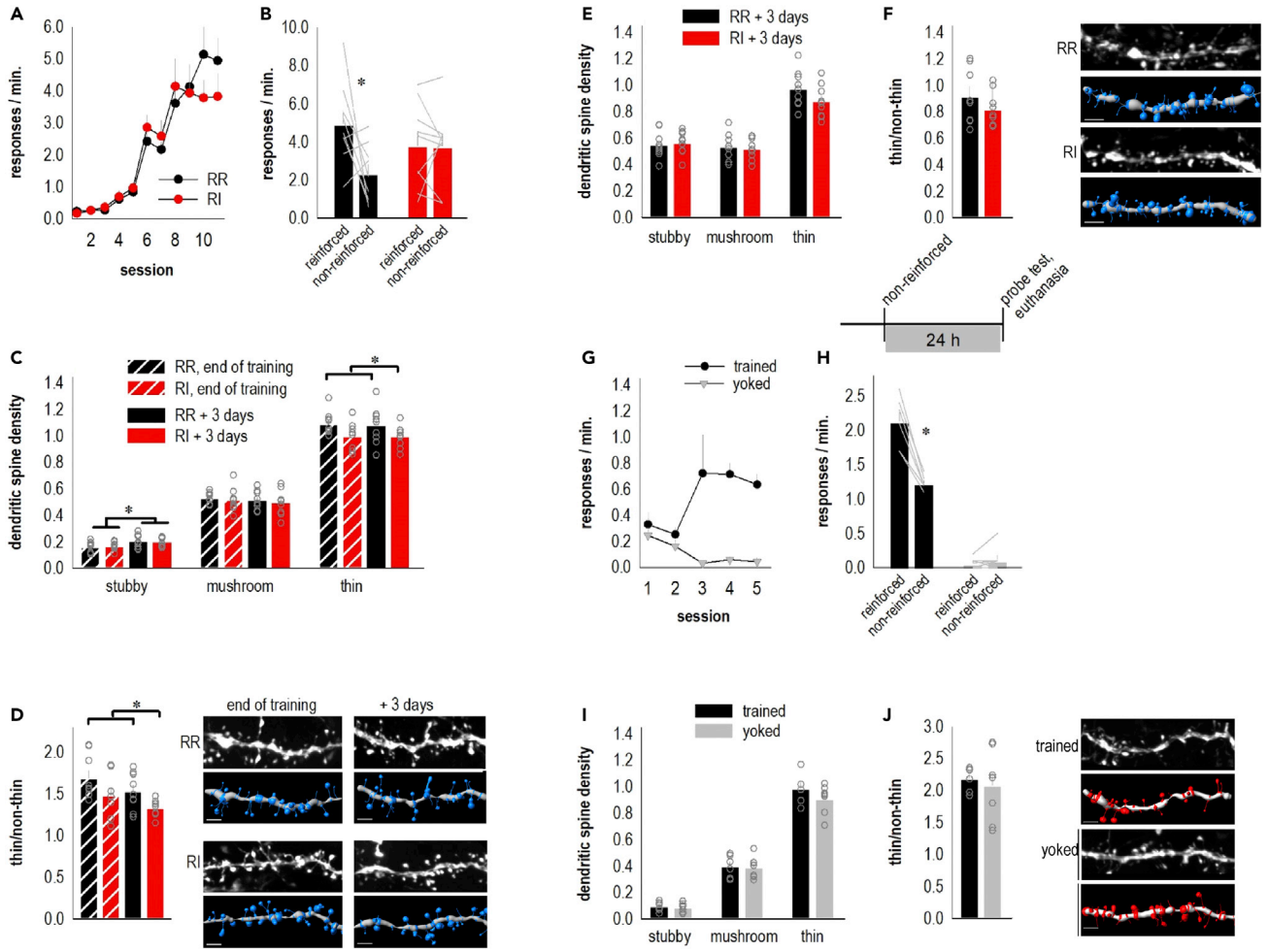

Figure 7. Habit-inducing training schedules remodel dendritic spines on PL neurons, resembling cocaine

(A and B) Mice were trained according to RR or RI schedules of reinforcement, resulting in (B) sensitivity and insensitivity to action-outcome contingency, respectively.

(C) RI training reduced thin-type dendritic spine densities (spines/μm) on excitatory PL neurons, anatomically defined as in Figure 3 (n = 8,9/group), relative to RR mice (n = 9/group). Brackets denote main effect of schedule, regardless of time of imaging.

(D) RI training also decreased the thin:non-thin spine type ratio. Brackets again denote main effect of schedule, regardless of time of imaging. Representative dendrites are adjacent.

(E and F) For anatomical comparison, dendrites on hippocampal CA1 neurons were imaged, with no group differences. Representative dendrites are adjacent.

(G) Separate mice were trained to respond for food according to ratio schedules of reinforcement. Other mice received food non-contingently at a rate yoked to a nose-poking pair throughout all phases of testing and thus did not have the opportunity to learn action-outcome associations.

(H) Nose-poking mice were sensitive to instrumental contingencies, preferring a reinforced behavior over one that ceased to be reinforced, as expected, while yoked mice did not respond, also as expected. Mice were euthanized for dendrite imaging (timeline at top).

(I and J) No differences in dendritic spine densities or ratios on excitatory PL neurons were identified (n = 6,7/group). Representative dendrites are adjacent. Bars and closed symbols: mean + SEMs. Open symbols and gray lines represent individual mice, *p < 0.05. Scale = 2 μm.

Esparza et al.[33] also reported thicker and longer postsynaptic densities 45 min following acute cocaine, focusing on layers II-IV. Anatomical considerations are worth noting, though. These investigators imaged neurons within the dorsal prefrontal cortex, which would typically refer to the anterior cingulate cortex and potentially M2. Thus, they concur with classical investigations indicating that psychostimulants cause dendritic spine proliferation in the anterior cingulate cortex.[34] Meanwhile, we took considerable pains to image dendritic spines in the PL in the rostral frontal pole, where it extends to the skull surface. It has distinct inputs and outputs relative to the anterior cingulate cortex[35–37] and also suffers dendritic spine and synaptic marker loss and hypo-activity following cocaine.[38–43]

Dendritic spines can be classified by their shape, which corresponds with their function, so we took advantage of high-fidelity *ex vivo* images from separate mice to reconstruct and classify dendritic spines. Thin-type spines are labile extensions that may or may not include synapses,[18,19] and the ratio of thin:non-thin spines rapidly decreased with only a single cocaine injection, again consistent with the time course of disrupted memory. In other investigations, a single cocaine injection rapidly (within 2 h) minimized perineuronal nets, increased inhibitory synapse markers, and decreased the excitability of fast-spiking interneurons in the PL.[44] Acute cocaine can also increase or decrease cofilin phosphorylation, depending on an organism's prior experience with cocaine and/or stressors.[33,45] These patterns are notable because cofilin is a fundamental actin-binding factor that regulates actin filaments, and its activity is terminated by phosphorylation.[46] Constitutively inactive cofilin can decrease dendritic spine protrusion length,[47] which occurs when spines are being eliminated, and cofilin inactivation *in vivo* is associated with stress-related dendrite atrophy.[48] Cocaine rapidly inactivated cofilin here, likely contributing to cocaine-induced destabilization of dendritic spines.

Notably, the cocaine-induced elevation in phospho-cofilin documented here appears to be a transient response to cocaine, given that we detected only moderate changes following repeated cocaine or repeated cocaine + drug washout. Instead, phosphorylation of cortactin, which stimulates the Arp2/3 complex and promotes branching of new actin filaments,[49,50] was elevated with repeated cocaine—one potential mechanism by which repeated cocaine persistently disrupts spine dynamics in the PL.[38]

Schedules of reinforcement that prompt inflexible behavior modify dendritic spine densities in the PL

A common notion is that addictive drugs usurp innate learning and memory processes. Following this logic, training mice to use response-inflexible action strategies might recapitulate the structural effects of cocaine. We capitalized on interval schedules of reinforcement that cause rodents to favor habit-based response strategies by weakening the predictive relationship between actions and outcomes.[26] Interval-trained mice generated the same number of responses as ratio-trained mice but were insensitive to changes in instrumental contingency, as expected. They also had fewer thin-type dendritic spines on excitatory pyramidal neurons in the PL, similar to the effects of cocaine, which reduced the ratio of thin:non-thin spines. Given that thin-type spines are labile, even referred to as "learning spines",[18] and can contain synapses, their presence may support PL control over behavior. By extension, constraint on thin-type spine presence may be a mechanism by which the PL yields control over reward-seeking behavior to brain regions that support competing habit-based response strategies (*e.g.*, the infralimbic prefrontal cortex and dorsolateral striatum[51]).

One possible alternative explanation was that training conditions that promote behavioral flexibility *stimulate* thin-type dendritic spinogenesis (as opposed to habit-inducing schedules *reducing* thin-type spine densities). However, PL neurons from response-flexible mice did not obviously differ from yoked control mice, which received the same handling and food but never learned to respond for food reinforcers. Thus, ratio training did not obviously remodel PL neurons, at least in a way that was detectable upon the *expression* of action-outcome learning. Consistent with this pattern, another manuscript reported modest reductions in specifically mushroom-shaped spines in the PL during new action-outcome learning. This modification was activity dependent and short lived, not detectable at later time points.[11] We suggest that cocaine causes atypical spine turnover in the PL, disrupting new learning.

Limitations of study

It is important to acknowledge that dendritic spine densities in our *in vivo* experiments are lower than those in our *ex vivo* experiments. This pattern is attributable to only being able to visually access very rostral and distal dendritic segments near the pial surface for *in vivo* imaging, where dendritic spine densities are typically low.[52,53] Another consideration is that our baseline turnover rates are higher than those reported by others,[25,54] which is likely attributable to difficulty in imaging neurons within the PL, given close proximity to the superior sagittal sinus and other major blood vessels. Motion of the brain would sometimes cause small portions of dendritic segments to shift out of the plane of focus at one time point and reappear in the next time point, artificially inflating turnover rates. Importantly, this inflation impacted both drug conditions and thus is unlikely to account for differences between them.

Another consideration is that ketamine was used as an anesthetic. Sub-anesthetic levels modify dendritic spine densities in frontal cortical regions, but notably, these actions require multiple hours, extending

beyond our imaging window.[55,56] Meanwhile, anesthetic levels appear to affect filopodia but leave spine dynamics intact,[57] so we do not believe ketamine had major impact on our findings. Nevertheless, the increasing availability of deep-brain imaging methods is making these kinds of experiments more feasible even in awake behaving mice. These technologies will allow investigators to circumvent concerns regarding anesthetics or region of PL that can be imaged, important because only the rostral pole is available for visualization through the thinned skull, while few *ex vivo* investigations (including our own) exclusively image this far rostrally. While we observed thin-type spine attrition with cocaine throughout, *which* connections are affected will depend on the rostro-caudal positioning of a given PL neuron (*e.g.*, see[58]).

We believe that further investigation is important because individuals suffering from drug misuse can suffer from an inability to plan forward, and they experience a narrowing of the likely environmental complexities that could occur as a result of their actions.[59] Without cognitive investment in considering the various outcomes of one's behaviors, one defers to "what I always have done," potentially propelling drug seeking and precipitating problematic drug use. Our findings suggest that modifications in neural structure may be a mechanism, and they lay the groundwork for experiments in which spine structures could be selectively manipulated to establish *causal relationships* with behavioral outcomes.

STAR★METHODS

Detailed methods are provided in the online version of this paper and include the following:

- KEY RESOURCES TABLE
- RESOURCE AVAILABILITY
  - Lead contact
  - Materials availability
  - Data and code availability
- EXPERIMENTAL MODEL AND SUBJECT DETAILS
- METHOD DETAILS
  - Instrumental response training
  - Test of response flexibility
  - Yoked comparator groups
  - Random ratio (RR) vs. random interval (RI) training
  - Intracranial surgery
  - *In vivo* dendritic spine imaging and analysis
  - *Ex vivo* dendritic spine imaging and analysis
  - Dendritic spine reconstruction
  - Western blotting
  - Drug injections and timing
  - Clozapine N-oxide (CNO)
- QUANTIFICATION AND STATISTICAL ANALYSIS

ACKNOWLEDGMENTS

This work was supported by NIH MH117103, DA034808, DA044297, and DA051184, and the Emory University Research Council in conjunction with the National Center for Advancing Translational Sciences of the National Institutes of Health under award number UL1TR002378. The Emory National Primate Research Center is supported by the Office of Research Infrastructure Programs/OD P51OD011132. We thank the Children's Healthcare of Atlanta and Emory University's Pediatric Integrated Cellular Imaging Core, Ms. Yong Yang, Ms. Courtni Andrews, Ms. Hayley Arrowood, and Dr. R. Jude Samulski of the UNC Viral Vector for their critical assistance. We thank Aylet Allen for preparing the graphical abstract. We thank Dr. Gary Bassell for generous resource sharing.

AUTHOR CONTRIBUTIONS

Conceptualization and methodology, M.K.S., A.M.S., and S.L.G.; Investigation, M.K.S., A.M.S., and H.W.K.; Writing, M.K.S., A.M.S., and S.L.G.; Funding acquisition, M.K.S. and S.L.G.; Supervision, S.L.G.

DECLARATION OF INTERESTS

The authors declare no competing interests.

INCLUSION AND DIVERSITY

We worked to ensure sex balance in the selection of non-human subjects. One or more of the authors of this paper self-identifies as an underrepresented ethnic minority in their field of research or within their geographical location. One or more of the authors of this paper self-identifies as a member of the LGBTQIA+ community. One or more of the authors of this paper received support from a program designed to increase minority representation in their field of research. While citing references scientifically relevant for this work, we also actively worked to promote gender balance in our reference list.

Received: July 7, 2022
Revised: January 2, 2023
Accepted: February 15, 2023
Published: February 20, 2023

REFERENCES

1. Euston, D.R., Gruber, A.J., and McNaughton, B.L. (2012). The role of medial prefrontal cortex in memory and decision making. Neuron *76*, 1057–1070. https://doi.org/10.1016/j.neuron.2012.12.002.

2. Uylings, H.B.M., Groenewegen, H.J., and Kolb, B. (2003). Do rats have a prefrontal cortex? Behav. Brain Res. *146*, 3–17. https://doi.org/10.1016/j.bbr.2003.09.028.

3. Balleine, B.W., and Dickinson, A. (1998). Goal-directed instrumental action: contingency and incentive learning and their cortical substrates. Neuropharmacology *37*, 407–419. https://doi.org/10.1016/s0028-3908(98)00033-1.

4. Corbit, L.H., and Balleine, B.W. (2003). The role of prelimbic cortex in instrumental conditioning. Behav. Brain Res. *146*, 145–157. https://doi.org/10.1016/j.bbr.2003.09.023.

5. Killcross, S., and Coutureau, E. (2003). Coordination of actions and habits in the medial prefrontal cortex of rats. Cerebr. Cortex *13*, 400–408. https://doi.org/10.1093/cercor/13.4.400.

6. Woon, E.P., Sequeira, M.K., Barbee, B.R., and Gourley, S.L. (2020). Involvement of the rodent prelimbic and medial orbitofrontal cortices in goal-directed action: a brief review. J. Neurosci. Res. *98*, 1020–1030. https://doi.org/10.1002/jnr.24567.

7. Shipman, M.L., Trask, S., Bouton, M.E., and Green, J.T. (2018). Inactivation of prelimbic and infralimbic cortex respectively affects minimally-trained and extensively-trained goal-directed actions. Neurobiol. Learn. Mem. *155*, 164–172. https://doi.org/10.1016/j.nlm.2018.07.010.

8. Ostlund, S.B., and Balleine, B.W. (2005). Lesions of medial prefrontal cortex disrupt the acquisition but not the expression of goal-directed learning. J. Neurosci. *25*, 7763–7770. https://doi.org/10.1523/JNEUROSCI.1921-05.2005.

9. Hart, G., Bradfield, L.A., and Balleine, B.W. (2018). Prefrontal corticostriatal disconnection blocks the acquisition of goal-directed action. J. Neurosci. *38*, 1311–1322. https://doi.org/10.1523/JNEUROSCI.2850-17.2017.

10. Hart, G., Bradfield, L.A., Fok, S.Y., Chieng, B., and Balleine, B.W. (2018). The bilateral prefronto-striatal pathway is necessary for learning new goal-directed actions. Curr. Biol. *28*, 2218–2229.e7. https://doi.org/10.1016/j.cub.2018.05.028.

11. Swanson, A.M., DePoy, L.M., and Gourley, S.L. (2017). Inhibiting Rho kinase promotes goal-directed decision making and blocks habitual responding for cocaine. Nat. Commun. *8*, 1861. https://doi.org/10.1038/s41467-017-01915-4.

12. Gourley, S.L., and Taylor, J.R. (2016). Going and stopping: dichotomies in behavioral control by the prefrontal cortex. Nat. Neurosci. *19*, 656–664. https://doi.org/10.1038/nn.4275.

13. Everitt, B.J., and Robbins, T.W. (2016). Drug addiction: updating actions to habits to compulsions ten years on. Annu. Rev. Psychol. *67*, 23–50. https://doi.org/10.1146/annurev-psych-122414-033457.

14. Ersche, K.D., Gillan, C.M., Jones, P.S., Williams, G.B., Ward, L.H.E., Luijten, M., de Wit, S., Sahakian, B.J., Bullmore, E.T., and Robbins, T.W. (2016). Carrots and sticks fail to change behavior in cocaine addiction. Science *352*, 1468–1471. https://doi.org/10.1126/science.aaf3700.

15. Gourley, S.L., Olevska, A., Gordon, J., and Taylor, J.R. (2013). Cytoskeletal determinants of stimulus-response habits. J. Neurosci. *33*, 11811–11816. https://doi.org/10.1523/JNEUROSCI.1034-13.2013.

16. Miles, F.J., Everitt, B.J., and Dickinson, A. (2003). Oral cocaine seeking by rats: action or habit? Behav. Neurosci. *117*, 927–938. https://doi.org/10.1037/0735-7044.117.5.927.

17. LeBlanc, K.H., Maidment, N.T., and Ostlund, S.B. (2013). Repeated cocaine exposure facilitates the expression of incentive motivation and induces habitual control in rats. PLoS One *8*, e61355. https://doi.org/10.1371/journal.pone.0061355.

18. Bourne, J., and Harris, K.M. (2007). Do thin spines learn to be mushroom spines that remember? Curr. Opin. Neurobiol. *17*, 381–386. https://doi.org/10.1016/j.conb.2007.04.009.

19. Berry, K.P., and Nedivi, E. (2017). Spine dynamics: are they all the same? Neuron *96*, 43–55. https://doi.org/10.1016/j.neuron.2017.08.008.

20. Hernandez, P.J., and Abel, T. (2008). The role of protein synthesis in memory consolidation: progress amid decades of debate. Neurobiol. Learn. Mem. *89*, 293–311. https://doi.org/10.1016/j.nlm.2007.09.010.

21. Bradfield, L.A., Dezfouli, A., van Holstein, M., Chieng, B., and Balleine, B.W. (2015). Medial orbitofrontal cortex mediates outcome retrieval in partially observable task situations. Neuron *88*, 1268–1280. https://doi.org/10.1016/j.neuron.2015.10.044.

22. Gomez, J.L., Bonaventura, J., Lesniak, W., Mathews, W.B., Sysa-Shah, P., Rodriguez, L.A., Ellis, R.J., Richie, C.T., Harvey, B.K., Dannals, R.F., et al. (2017). Chemogenetics revealed: DREADD occupancy and activation via converted clozapine. Science *357*, 503–507. https://doi.org/10.1126/science.aan2475.

23. Treccani, G., Ardalan, M., Chen, F., Musazzi, L., Popoli, M., Wegener, G., Nyengaard, J.R., and Müller, H.K. (2019). S-ketamine reverses hippocampal dendritic spine deficits in flinders sensitive line rats within 1 h of administration. Mol. Neurobiol. *56*, 7368–7379. https://doi.org/10.1007/s12035-019-1613-3.

24. Toda, S., Shen, H.-W., Peters, J., Cagle, S., and Kalivas, P.W. (2006). Cocaine increases actin cycling: effects in the reinstatement model of drug seeking. J. Neurosci. *26*, 1579–1587. https://doi.org/10.1523/JNEUROSCI.4132-05.2006.

25. Liston, C., and Gan, W.B. (2011). Glucocorticoids are critical regulators of dendritic spine development and plasticity in vivo. Proc. Natl. Acad. Sci. USA *108*, 16074–16079. https://doi.org/10.1073/pnas.1110444108.

26. de Wit, S., and Dickinson, A. (2009). Associative theories of goal-directed behaviour: a case for animal-human translational models. Psychol. Res. *73*, 463–476. https://doi.org/10.1007/s00426-009-0230-6.

27. Whyte, A.J., Kietzman, H.W., Swanson, A.M., Butkovich, L.M., Barbee, B.R., Bassell, G.J., Gross, C., and Gourley, S.L. (2019). Reward-related expectations trigger dendritic spine plasticity in the mouse ventrolateral orbitofrontal cortex. J. Neurosci. *39*, 4595–4605. https://doi.org/10.1523/JNEUROSCI.2031-18.2019.

28. Runge, K., Cardoso, C., and de Chevigny, A. (2020). Dendritic spine plasticity: function and mechanisms. Front. Synaptic Neurosci. *12*, 36. https://doi.org/10.3389/fnsyn.2020.00036.

29. Moorman, D.E., James, M.H., McGlinchey, E.M., and Aston-Jones, G. (2015). Differential roles of medial prefrontal subregions in the regulation of drug seeking. Brain Res. *1628*, 130–146. https://doi.org/10.1016/j.brainres.2014.12.024.

30. Alcaraz, F., Fresno, V., Marchand, A.R., Kremer, E.J., Coutureau, E., and Wolff, M. (2018). Thalamocortical and corticothalamic pathways differentially contribute to goal-directed behaviors in the rat. Elife *7*, e32517. https://doi.org/10.7554/eLife.32517.

31. Kuroda, M., Murakami, K., Igarashi, H., and Okada, A. (1996). The convergence of axon terminals from the mediodorsal thalamic nucleus and ventral tegmental area on pyramidal cells in layer V of the rat prelimbic cortex. Eur. J. Neurosci. *8*, 1340–1349. https://doi.org/10.1111/j.1460-9568.1996.tb01596.x.

32. Muñoz-Cuevas, F.J., Athilingam, J., Piscopo, D., and Wilbrecht, L. (2013). Cocaine-induced structural plasticity in frontal cortex correlates with conditioned place preference. Nat. Neurosci. *16*, 1367–1369. https://doi.org/10.1038/nn.3498.

33. Esparza, M.A., Bollati, F., Garcia-Keller, C., Virgolini, M.B., Lopez, L.M., Brusco, A., Shen, H.-W., Kalivas, P.W., and Cancela, L.M. (2012). Stress-induced sensitization to cocaine: actin cytoskeleton remodeling within mesocorticolimbic nuclei. Eur. J. Neurosci. *36*, 3103–3117. https://doi.org/10.1111/j.1460-9568.2012.08239.x.

34. DePoy, L.M., and Gourley, S.L. (2015). Synaptic cytoskeletal plasticity in the prefrontal cortex following psychostimulant exposure. Traffic *16*, 919–940. https://doi.org/10.1111/tra.12295.

35. Zhang, S., Xu, M., Chang, W.-C., Ma, C., Hoang Do, J.P., Jeong, D., Lei, T., Fan, J.L., and Dan, Y. (2016). Organization of long-range inputs and outputs of frontal cortex for top-down control. Nat. Neurosci. *19*, 1733–1742. https://doi.org/10.1038/nn.4417.

36. Anastasiades, P.G., and Carter, A.G. (2021). Circuit organization of the rodent medial prefrontal cortex. Trends Neurosci. *44*, 550–563. https://doi.org/10.1016/j.tins.2021.03.006.

37. Heidbreder, C.A., and Groenewegen, H.J. (2003). The medial prefrontal cortex in the rat: evidence for a dorso-ventral distinction based upon functional and anatomical characteristics. Neurosci. Biobehav. Rev. *27*, 555–579. https://doi.org/10.1016/j.neubiorev.2003.09.003.

38. Radley, J.J., Anderson, R.M., Cosme, C.V., Glanz, R.M., Miller, M.C., Romig-Martin, S.A., and LaLumiere, R.T. (2015). The contingency of cocaine administration accounts for structural and functional medial prefrontal deficits and increased adrenocortical activation. J. Neurosci. *35*, 11897–11910. https://doi.org/10.1523/JNEUROSCI.4961-14.2015.

39. Rasakham, K., Schmidt, H.D., Kay, K., Huizenga, M.N., Calcagno, N., Pierce, R.C., Spires-Jones, T.L., and Sadri-Vakili, G. (2014). Synapse density and dendritic complexity are reduced in the prefrontal cortex following seven days of forced abstinence from cocaine self-administration. PLoS One *9*, e102524. https://doi.org/10.1371/journal.pone.0102524.

40. Caffino, L., Giannotti, G., Malpighi, C., Racagni, G., and Fumagalli, F. (2015). Short-term withdrawal from developmental exposure to cocaine activates the glucocorticoid receptor and alters spine dynamics. Eur. Neuropsychopharmacol *25*, 1832–1841. https://doi.org/10.1016/j.euroneuro.2015.05.002.

41. Zhu, W., Ge, X., Gao, P., Li, M., Guan, Y., and Guan, X. (2018). Adolescent cocaine exposure induces prolonged synaptic modifications in medial prefrontal cortex of adult rats. Brain Struct. Funct. *223*, 1829–1838. https://doi.org/10.1007/s00429-017-1590-0.

42. Shi, P., Nie, J., Liu, H., Li, Y., Lu, X., Shen, X., Ge, F., Yuan, T.-F., and Guan, X. (2019). Adolescent cocaine exposure enhances the GABAergic transmission in the prelimbic cortex of adult mice. Faseb. J. *33*, 8614–8622. https://doi.org/10.1096/fj.201802192RR.

43. Chen, B.T., Yau, H.-J., Hatch, C., Kusumoto-Yoshida, I., Cho, S.L., Hopf, F.W., and Bonci, A. (2013). Rescuing cocaine-induced prefrontal cortex hypoactivity prevents compulsive cocaine seeking. Nature *496*, 359–362. https://doi.org/10.1038/nature12024.

44. Slaker, M.L., Jorgensen, E.T., Hegarty, D.M., Liu, X., Kong, Y., Zhang, F., Linhardt, R.J., Brown, T.E., Aicher, S.A., and Sorg, B.A. (2018). Cocaine exposure modulates perineuronal nets and synaptic excitability of fast-spiking interneurons in the medial prefrontal cortex. eNeuro *5*. ENEURO.0221-18.2018. https://doi.org/10.1523/ENEURO.0221-18.2018.

45. Shen, H.-W., Toda, S., Moussawi, K., Bouknight, A., Zahm, D.S., and Kalivas, P.W. (2009). Altered dendritic spine plasticity in cocaine-withdrawn rats. J. Neurosci. *29*, 2876–2884. https://doi.org/10.1523/JNEUROSCI.5638-08.2009.

46. Ono, S. (2003). Regulation of actin filament dynamics by actin depolymerizing factor/cofilin and actin-interacting protein 1: new blades for twisted filaments. Biochemistry *42*, 13363–13370. https://doi.org/10.1021/bi034600x.

47. Shi, Y., Pontrello, C.G., DeFea, K.A., Reichardt, L.F., and Ethell, I.M. (2009). Focal adhesion kinase acts downstream of EphB receptors to maintain mature dendritic spines by regulating cofilin activity. J. Neurosci. *29*, 8129–8142. https://doi.org/10.1523/JNEUROSCI.4681-08.2009.

48. Shapiro, L.P., Parsons, R.G., Koleske, A.J., and Gourley, S.L. (2017). Differential expression of cytoskeletal regulatory factors in the adolescent prefrontal cortex: implications for cortical development. J. Neurosci. Res. *95*, 1123–1143. https://doi.org/10.1002/jnr.23960.

49. Uruno, T., Liu, J., Zhang, P., Fan, Y., Egile, C., Li, R., Mueller, S.C., and Zhan, X. (2001). Activation of Arp2/3 complex-mediated actin polymerization by cortactin. Nat. Cell Biol. *3*, 259–266. https://doi.org/10.1038/35060051.

50. Courtemanche, N., Gifford, S.M., Simpson, M.A., Pollard, T.D., and Koleske, A.J. (2015). Abl2/Abl-related gene stabilizes actin filaments, stimulates actin branching by actin-related protein 2/3 complex, and promotes actin filament severing by cofilin. J. Biol. Chem. *290*, 4038–4046. https://doi.org/10.1074/jbc.M114.608117.

51. Malvaez, M. (2020). Neural substrates of habit. J. Neurosci. Res. *98*, 986–997. https://doi.org/10.1002/jnr.24552.

52. Duan, H., Wearne, S.L., Rocher, A.B., Macedo, A., Morrison, J.H., and Hof, P.R. (2003). Age-related dendritic and spine changes in corticocortically projecting neurons in macaque monkeys. Cerebr. Cortex *13*, 950–961. https://doi.org/10.1093/cercor/13.9.950.

53. Benavides-Piccione, R., Fernaud-Espinosa, I., Robles, V., Yuste, R., and DeFelipe, J. (2013). Age-based comparison of human dendritic spine structure using complete three-dimensional reconstructions. Cerebr. Cortex *23*, 1798–1810. https://doi.org/10.1093/cercor/bhs154.

54. Wilbrecht, L., Holtmaat, A., Wright, N., Fox, K., and Svoboda, K. (2010). Structural plasticity underlies experience-dependent functional plasticity of cortical circuits. J. Neurosci. *30*, 4927–4932. https://doi.org/10.1523/JNEUROSCI.6403-09.2010.

55. Moda-Sava, R.N., Murdock, M.H., Parekh, P.K., Fetcho, R.N., Huang, B.S., Huynh, T.N., Witztum, J., Shaver, D.C., Rosenthal, D.L., Alway, E.J., et al. (2019). Sustained rescue of prefrontal circuit dysfunction by antidepressant-induced spine formation. Science *364*, eaat8078. https://doi.org/10.1126/science.aat8078.

56. Wu, M., Minkowicz, S., Dumrongprechachan, V., Hamilton, P., and Kozorovitskiy, Y. (2021). Ketamine rapidly enhances glutamate-evoked dendritic spinogenesis in medial prefrontal cortex through dopaminergic mechanisms. Biol. Psychiatr. *89*, 1096–1105. https://doi.org/10.1016/j.biopsych.2020.12.022.

57. Yang, G., Chang, P.C., Bekker, A., Blanck, T.J.J., and Gan, W.-B. (2011). Transient effects of anesthetics on dendritic spines and filopodia in the living mouse cortex.

Anesthesiology *115*, 718–726. https://doi.org/10.1097/ALN.0b013e318229a660.

58. Jay, T.M., and Witter, M.P. (1991). Distribution of hippocampal CA1 and subicular efferents in the prefrontal cortex of the rat studied by means of anterograde transport of Phaseolus vulgaris-leucoagglutinin. J. Comp. Neurol. *313*, 574–586. https://doi.org/10.1002/cne.903130404.

59. Ognibene, D., Fiore, V.G., and Gu, X. (2019). Addiction beyond pharmacological effects: the role of environment complexity and bounded rationality. Neural Network. *116*, 269–278. https://doi.org/10.1016/j.neunet.2019.04.022.

60. Feng, G., Mellor, R.H., Bernstein, M., Keller-Peck, C., Nguyen, Q.T., Wallace, M., Nerbonne, J.M., Lichtman, J.W., and Sanes, J.R. (2000). Imaging neuronal subsets in transgenic mice expressing multiple spectral variants of GFP. Neuron *28*, 41–51. https://doi.org/10.1016/s0896-6273(00)00084-2.

61. Gourley, S.L., Swanson, A.M., Jacobs, A.M., Howell, J.L., Mo, M., Dileone, R.J., Koleske, A.J., and Taylor, J.R. (2012). Action control is mediated by prefrontal BDNF and glucocorticoid receptor binding. Proc. Natl. Acad. Sci. USA *109*, 20714–20719. https://doi.org/10.1073/pnas.1208342109.

62. Butkovich, L.M., DePoy, L.M., Allen, A.G., Shapiro, L.P., Swanson, A.M., and Gourley, S.L. (2015). Adolescent-onset GABAA α1 silencing regulates reward-related decision making. Eur. J. Neurosci. *42*, 2114–2121. https://doi.org/10.1111/ejn.12995.

63. Gremel, C.M., and Costa, R.M. (2013). Orbitofrontal and striatal circuits dynamically encode the shift between goal-directed and habitual actions. Nat. Commun. *4*, 2264. https://doi.org/10.1038/ncomms3264.

64. Yang, G., Pan, F., Parkhurst, C.N., Grutzendler, J., and Gan, W.-B. (2010). Thinned-skull cranial window technique for long-term imaging of the cortex in live mice. Nat. Protoc. *5*, 201–208. https://doi.org/10.1038/nprot.2009.222.

65. Gourley, S.L., Swanson, A.M., and Koleske, A.J. (2013). Corticosteroid-induced neural remodeling predicts behavioral vulnerability and resilience. J. Neurosci. *33*, 3107–3112. https://doi.org/10.1523/JNEUROSCI.2138-12.2013.

66. Swanger, S.A., Yao, X., Gross, C., and Bassell, G.J. (2011). Automated 4D analysis of dendritic spine morphology: applications to stimulus-induced spine remodeling and pharmacological rescue in a disease model. Mol. Brain *4*, 38. https://doi.org/10.1186/1756-6606-4-38.

67. Witte, R.S., and Witte, J.S. (2017). Statistics (John Wiley & Sons).

STAR★METHODS

KEY RESOURCES TABLE

REAGENT or RESOURCE	SOURCE	IDENTIFIER
Antibodies		
Rabbit anti c-fos	Santa Cruz Biotechnology	Cat. # sc-52; RRID:AB_2106783
Rabbit anti p-cofilin	Cell Signaling Technology	Cat. # 3311S; RRID:AB_330238
Rabbit anti cofilin	ECM Biosciences	Cat. # CP1131; RRID:AB_2260620
Rabbit anti p-adducin	Millipore Sigma	Cat. # 06-820; RRID:AB_310256
Mouse anti adducin	Santa Cruz Biotechnology	Cat. # sc-376063; RRID:AB_10987642
Rabbit anti p-FAK	Abcam	Cat. # ab81298; RRID:AB_1640500
Rabbit anti FAK	Cell Signaling Technology	Cat. # 3285S; RRID:AB_2269034
Rabbit anti p-Pyk2	Cell Signaling Technology	Cat. # 3291S; RRID:AB_2300530
Rabbit anti Pyk2	Cell Signaling Technology	Cat. # 3292S; RRID:AB_2174097
Rabbit anti p-ROCK2	GeneTex	Cat. # GTX122651; RRID:AB_2560946
Rabbit anti ROCK2	Abcam	Cat. # ab71598; RRID:AB_1566688
Rabbit anti p-LIMK	Cell Signaling Technology	Cat. # 3841S; RRID:AB_2136943
Rabbit anti LIMK	Santa Cruz Biotechnology	Cat. # sc-5577; RRID:AB_2265804
Rabbit anti BDNF	Abcam	Cat. # ab108319; RRID:AB_10862052
Rabbit anti p-TrkB	Cell Signaling Technology	Cat. # 4621S; RRID:AB_916186
Rabbit anti TrkB	Cell Signaling Technology	Cat. # 4603S; RRID:AB_2155125
Rabbit anti p-ERK	Cell Signaling Technology	Cat. # 9101S; RRID:AB_331646
Rabbit anti ERK	Cell Signaling Technology	Cat. # 9102S; RRID:AB_330744
Rabbit anti p-Cortactin	Cell Signaling Technology	Cat. # 4569S; RRID:AB_2276917
Mouse anti Cortactin	Santa Cruz Biotechnology	Cat. # sc-55578; RRID:AB_831186
Bacterial and virus strains		
AAV5-CaMKII-HA-hM4D(Gi)-IRES-mCitrine	UNC Viral Vector Core	N/A
AAV5-CaMKII-GFP	UNC Viral Vector Core	N/A
Chemicals, peptides, and recombinant proteins		
Clozapine-N-oxide	Sigma-Aldrich	Cat. # C0832
Cocaine hydrochloride	Sigma-Aldrich	Cat. # C5776
Experimental models: Organisms/strains		
Mouse: Thy1-YFP-H	The Jackson Laboratory	Stock #003782
Software and algorithms		
Imaris v.8	Oxford Instruments	http://imaris.oxinst.com
ImageJ	Wayne Rasband	http://imagej.nih.gov/ij/
SPSS v.28	IBM	http://www.ibm.com/products/spss-statistics
SigmaPlot v.15	Systat	https://systatsoftware.com/sigmaplot/

RESOURCE AVAILABILITY

Lead contact

Further information and requests for resources should be directed to the lead contact, Shannon Gourley (shannon.l.gourley@emory.edu).

Materials availability

This study did not generate new unique reagents.

Data and code availability

- Data reported in this paper may be shared by the lead contact upon request.
- This paper does not report original code.
- Any additional information required to reanalyze the data reported in this paper is available from the lead contact upon request.

EXPERIMENTAL MODEL AND SUBJECT DETAILS

Mice were transgenic mice expressing *Thy1*-YFP-H[60] and back-crossed onto a C57BL/6 background, ≥6 weeks old. These mice express YFP in layer V excitatory cortical neurons, enabling their visualization. We used both sexes except for *in vivo* imaging experiments: While we were successful in imaging PL dendritic spines in males, we had significantly less success in females. Bleeding from the vessels in and around the thinned skull area was much more frequent and difficult to stop, both during the skull-thinning procedure and once 2-photon imaging began. This challenge decreased image quality over successive time points and reduced the number of dendritic spines detected. Thus, females are not included in *in vivo* dendritic spine imaging experiments. Mice were maintained on a 12-h light cycle (0700-0800 on) and provided food and water *ad libitum* except during instrumental conditioning when body weights were reduced to ~87-93% of baseline to motivate food-reinforced responding. All procedures were performed in accordance with NIH Guidelines for the Care and Use of Laboratory Animals and were approved by the Emory University IACUC.

METHOD DETAILS

Instrumental response training

Mice were food-restricted to ~90-93% of their original body weights and trained to nose poke for food pellets (20 mg, Bio-Serv, Flemington, NJ) in Med-Associates operant conditioning chambers (St. Albans, VT). Chambers were equipped with two nose poke recesses and a separate food magazine. Responding was reinforced using a fixed ratio 1 (FR1) schedule wherein 30 pellets were available for responding on the 2 distinct nose poke recesses, resulting in 60 pellets/session. In initial experiments (Figure 1), mice were reinforced with two separate pellets (*e.g.*, left nose poke resulted in a sweetened grain pellet, while right nose poke resulted in a chocolate pellet). Subsequent experiments replicated the effects in Figure 1 with a single pellet being used and thus, in subsequent experiments, both nose pokes were reinforced with the same pellet (purified sweet grain), and response rates are represented as total nose pokes/min. Sessions ended when mice acquired all 60 pellets or at 135 min., whichever came first. In replication experiments, sessions ended when mice acquired all 60 pellets or at 70 min. for expediency. Mice acquired all reinforcers per session within 5-7 d of training.

Test of response flexibility

A test of response flexibility was used[11,61] (Figure 1A). In a 25-min. "reinforced" session, one nose poke aperture was occluded, and responding on the other aperture was reinforced using a variable ratio 2 schedule of reinforcement. In the 25-min. "non-reinforced" session, the opposite aperture was occluded, and reinforcers were delivered into the magazine at a rate matched to each animal's reinforcement rate from the previous session. Responses produced no programmed consequences. In this case, only ~7% of pellets are delivered (by chance) within 2 sec. following a response.[62] Thus, one response becomes significantly less predictive of reinforcement than the other. Sessions were counter-balanced between and within groups. The following day, both apertures were available during a 10-min. probe test conducted in extinction. The probe test was repeated the following day in our initial experiment to document the stability of response patterns. Preferential engagement of the response most likely to be reinforced is considered flexible responding.

The value of this task is that memory consolidation and retrieval occur during discrete times, allowing us to manipulate them individually. During the non-reinforced session, a familiar behavior is not reinforced, which should trigger new learning. Meanwhile, memory retrieval occurs the following day during a probe test, when mice must choose their response strategies.

Yoked comparator groups

In one experiment, mice were trained to acquire food reinforcers and tested as described above. Each mouse was paired with a sibling that was food-restricted and placed in a chamber for the same duration

daily, however pellets were instead delivered non-contingently at the same rate as acquired by the paired animal. For these animals, mice did not have the opportunity to learn about action consequences.

Random ratio (RR) vs. random interval (RI) training

In one experiment, we aimed to generate mice that utilize goal-directed, vs. habit-based, response strategies, while controlling for the number of responses generated. This goal can be accomplished by training mice according to different schedules of reinforcement. We adapted a protocol from.[63] Responding on one nose poke recess was reinforced with grain pellets, and sessions lasted up to 70 min. in duration. The first 6 sessions used an FR1 schedule of reinforcement, and mice were reinforced with up to 5, 15, 30, 30, and 30 pellets, respectively. Next, mice were split by matching response rates. They were then trained according to either 2 RR3 sessions, followed by 4 RR6 sessions (biasing responding towards a flexible strategy that is sensitive to instrumental contingencies), or 2 RI30-sec. sessions followed by 4 RI60-sec. sessions (biasing responding towards habits). 30 pellets were available per session. Finally, mice were tested in a session in which food was delivered non-contingently: In this case, pellets were delivered at a rate matched to each animal's reinforcement rate on the prior day of training. Responding was not reinforced. The following day, a 5-min. probe test was conducted in extinction, and response rates were compared to the last day of training.

Intracranial surgery

Mice were anesthetized with a 100 mg/kg ketamine/1 mg/kg xylazine mixture and then placed in a stereotaxic frame. With infusion needles centered at bregma, a hole was drilled in the skull corresponding to +2.0 AP, +/−0.1 ML, −2.8 DV. AAV5-CaMKII-HA-hM4D(Gi)-IRES-mCitrine or AAV5-CaMKII-GFP (UNC Viral Vector Core) were infused bilaterally (0.5 μl per hemisphere) over 5 min. with the needle left in place for an additional 5 min. Mice were sutured and allowed to recover for 3 weeks, allowing time for viral vector expression.

In vivo dendritic spine imaging and analysis

Thinned skull preparation

We adapted Gan's thinned skull approach[64] to image dendrites within the PL. Behaviorally-naïve YFP-expressing mice were anesthetized with a ketamine/xylazine mixture as above. Once mice were sedated, the head was shaved and ocular ointment was placed on the eyes, and mice were placed in a stereotaxic instrument. A scalpel was used to place a long midline incision in the scalp, and the two skin flaps were pulled back. At +2.8 mm anterior from Bregma, the PL sits directly below the skull and extends approximately 500 μm laterally from the midline. Once this area was marked, the mouse was removed from the stereotaxic instrument.

Next, the skin flaps were positioned to create a circular expanse of skull centered around the marked area. Cyanoacrylate glue was placed around the interior opening of a double-edged razor blade, which was then carefully centered over the marked area and placed in direct contact with the skull. The razor blade was then secured to a custom stage adapter for use under a dissecting microscope and on the 2-photon microscope.

Along the dorsal midline of the skull run major blood vessels that fill the space between the dorsal portions of the two hemispheres of the brain. The dorsal portion of the brain has a roughly triangle-shaped gap where this vessel and the surrounding bone sits. Instead of making a symmetric, round depression in the skull like one can use when imaging more lateral brain regions, we instead thinned the skull directly adjacent to the midline blood vessels and along the curvature of the skull. The goal was to produce a very thin layer of curved skull without disrupting the major vessel or any of its lateral projections.

The initial thinning of the skull was accomplished using a high-speed drill, and then a fine scalpel or hypodermic needle was used to manually scrape off the remaining skull to as thin as possible. Once this point was reached, the stage adapter and mouse were transferred to the 2-photon microscope for imaging.

2-photon imaging

Images were acquired on a Leica SP8 system equipped with a Coherent Chameleon Vision II laser tuned to 920 nm. Initial targeting was completed using the confocal scanner and a 488 nm line from an Argon laser.

A 25x 0.95 NA HCX IRAPO dipping objective and a HyD detector were used to acquire images. A 4x zoom was used, resulting in a pixel size of 0.065 μm, and a 0.5 μm step size. Laser power was set as low as possible while still enabling clear image acquisition. For each time point and for each mouse, 2 z-stacks of the same individual dendrite were acquired back-to-back, to minimize loss of image quality caused by motion artifacts like animal respiration. Each mouse was considered an independent sample. Overall, ~105 dendritic spines/mouse were quantified from dendritic segments within the acquired z-stack.

A challenge of imaging an area near the midline is that bleeding tends to begin spontaneously. Frequently, bleeding would occur partway through an experiment that could not be stopped, at which point the experiment was terminated, and any collected images were omitted from analysis.

After imaging was complete, the 2-photon laser was turned to high power and used to photobleach an area adjacent to the imaged area to allow for post-mortem confirmation of the region of interest. Respiration and anesthesia level were checked regularly throughout imaging, and additional anesthetic (20 mg/kg / 0.2 mg/kg ketamine/xylazine, *i.p.*) was administered if needed.

Ex vivo dendritic spine imaging and analysis

YFP-expressing mice were euthanized by rapid decapitation, with timing indicated in the figure timelines or legends. Brains were extracted and submerged in 4% paraformaldehyde for 48 h and then transferred to 30% w/v sucrose. 50 μm-thick sections were prepared on a microtome held at -15°C±1. Images were collected from the PL as outlined in Figure 3A and acquired on a Leica DM5500B microscope equipped with a spinning disk confocal (VisiTech International) and a Hamamatsu Orca R2 camera using a 100x 1.4 NA objective. Z-stacks of dendritic segments were acquired using a 0.1 μm step size. 5-8 dendrites per mouse were acquired bilaterally from independent neurons. The location of the imaged segments within target brain regions was confirmed by zooming out to a low magnification. Care was taken to image second-order or higher apical PL dendrites 50-150 μm from soma. For comparison, secondary apical dendrites located 150-250 μm from the somatic layer in dorsal hippocampal CA1 were also imaged. Dendrites were 15-25 μm in length. A single blinded user generated all images.

Dendritic spine reconstruction

The FilamentTracer module of Imaris (Bitplane AG) was used as described[65,66]: A dendritic segment 15-25 μm in length was drawn with the autodepth function. Dendritic spine head location was manually indicated, and FilamentTracer processing algorithms were used to calculate morphological parameters. A single blinded individual quantified all dendritic spines within a given experiment.

Western blotting

Mice were briefly anaesthetized by isoflurane and euthanized by decapitation. Brains were frozen at -80°C, then sectioned at 1 mm. A single experimenter centered a 1 mm corer around the PL for dissection. Tissue was homogenized by sonication, and protein content was measured by Bradford colorimetric assay. 10 μg of protein/sample was separated by SDS-PAGE on a 4-20% gradient tris-glycine stain-free gel (Bio-rad). Following transfer to PVDF membrane, membranes were blocked with 5% nonfat milk.

Primary antibodies are listed in Table 2. Membranes were incubated overnight and then in horseradish peroxidase-conjugated goat anti-rabbit (Vector; 1:5000) secondary antibody. Immunoreactivity was assessed using a chemiluminescence substrate (Pierce) and measured using a ChemiDoc Imager (Bio-rad). Protein signals were normalized to their corresponding total protein signal. Phospho-signals were normalized to the corresponding non-phosphorylated protein signals (which did not differ between groups), then to the control sample mean from the same membrane to control for variance between gels.

In one experiment, we assessed protein content at multiple time points following cocaine. One lane in the cofilin analyses was unexpectedly blank and excluded. For all western blots, samples were run at least twice to ensure replication. Each mouse contributed only a single value to statistical analyses. Molecular weights were confirmed by comparison to the Bio-Rad Precision Plus Protein Standard (catalog #161-0373) run on every gel.

Drug injections and timing

Mice were injected with cocaine hydrochloride (10 mg/kg, *i.p.*, in saline, Sigma) or saline. The timing of injections, testing, and euthanasia are depicted in timelines and/or figure legends. In behavioral experiments, injections were delivered immediately, 30 min., 4 h, or 19 h after a session in which pellets were delivered non-contingently, and mice were then returned to the home cage. The probe tests were conducted in the absence of any further injections. These experiments led us to focus on the effects of cocaine detectable within 30 min. after injection. In *in vivo* dendritic spine imaging experiments, mice were injected with saline, and dendritic spines were imaged for 30 min., then mice were injected with cocaine, and the same dendrites were imaged for an additional 30 min. For *ex vivo* imaging experiments, mice were injected with cocaine, then euthanized at 30 min. or at 24 h later for comparison.

In western blotting experiments, mice were injected with saline or cocaine (10 mg/kg, *i.p.*), then euthanized 30 min. later. As a comparator, we also generated mice that received repeated cocaine (30 mg/kg, *i.p.*), ketamine (30 mg/kg, *i.p.*), or saline. Mice were given a single injection daily for 14 d, then euthanized 30 min. or 7 d following the final injection.

Clozapine N-oxide (CNO)

CNO (Sigma) was delivered at a dose of 1 mg/kg, *i.p.*, dissolved in 2% DMSO and sterile saline. CNO was delivered immediately following the session in which pellets were delivered non-contingently, and mice were tested in the probe test the next day drug-free. All mice received CNO, regardless of condition, to equally expose animals to any unintended consequences of CNO.[22] Importantly, this dose does not by itself impact responding in this task.[27]

Throughout, systemic injections were delivered in a volume of 1 ml/100 g.

QUANTIFICATION AND STATISTICAL ANALYSIS

Nose poke rates were compared by ANOVA, with nose poke port and group as factors, and with repeated measures when appropriate. In the case of significant interactions, post-hoc comparisons were made with Tukey's tests, and results are indicated graphically. In the behavioral probe tests, an interaction between nose poke port and drug is required to conclude that a given drug affected decision-making strategies; note that in such cases of significant interaction effects, main effects can be misleading and are thus not reported.[67]

For western blot analyses, each mouse contributed a single value (each animal's mean value from multiple gels). Comparisons were made by unpaired t-tests or 2-factor (time x drug) ANOVA, as appropriate.

For *in vivo* dendritic spine analyses, densities were compared at 3 time points (immediately following injection, referred to as time 0, then 15 and 30 min. following injection) via 2-factor ANOVA (time x drug) with repeating measures. Turnover rates were calculated as the number of spines gained or lost relative to the total number of spines present *at the previous time point*,[25] generating turnover values for time points 15 and 30 min. These rates were then compared by 2-factor ANOVA (time x drug). Post-hoc comparisons were made with Tukey's tests.

For *ex vivo* dendritic spine analyses, each mouse contributed a single spine density per subtype (reflecting the average of all dendrites from that mouse). Densities were compared by unpaired t-test applied to each spine type or ANOVA with time of euthanasia as a factor. Thin/non-thin spine ratios were also calculated and compared by unpaired t-test or ANOVA as appropriate. In this analysis, 3 values were identified as falling >2 standard deviations of the mean and were considered outliers and excluded.

Throughout, SigmaStat and SPSS were used, and $p \leq 0.05$ was considered significant. Comparisons were 2-tailed. Throughout, sex was included as a variable; no sex differences (all $p > 0.1$) were noted. n values for each individual group are reported in the figure captions. The data in Figure 3E were not normally distributed, and Kruskal-Wallis ANOVA on Ranks was applied.